Title

CORE-LEVEL PHOTOELECTRON AND AUGER SHAPE-RESONANCE PHENOMENA IN CO, CO2, CF2, AND OCS

Author

Truesdale, CM.

Publication Date

1983-10-01

LBL-15540
Preprint

Lawrence Berkeley Laboratory
UNIVERSITY OF CALIFORNIA

Materials & Molecular
Research Division

Submitted to the Journal of Chemical Physics

CORE-LEVEL PHOTOELECTRON AND AUGER SHAPE-RESONANCE PHENOMENA IN CO, CO_2, CF_4, AND OCS

C.M. Truesdale, D.W. Lindle, P.H. Kobrin,
U.E. Becker, H.G. Kerkhoff, P.A. Heimann,
T.A. Ferrett, and D.A. Shirley

October 1983

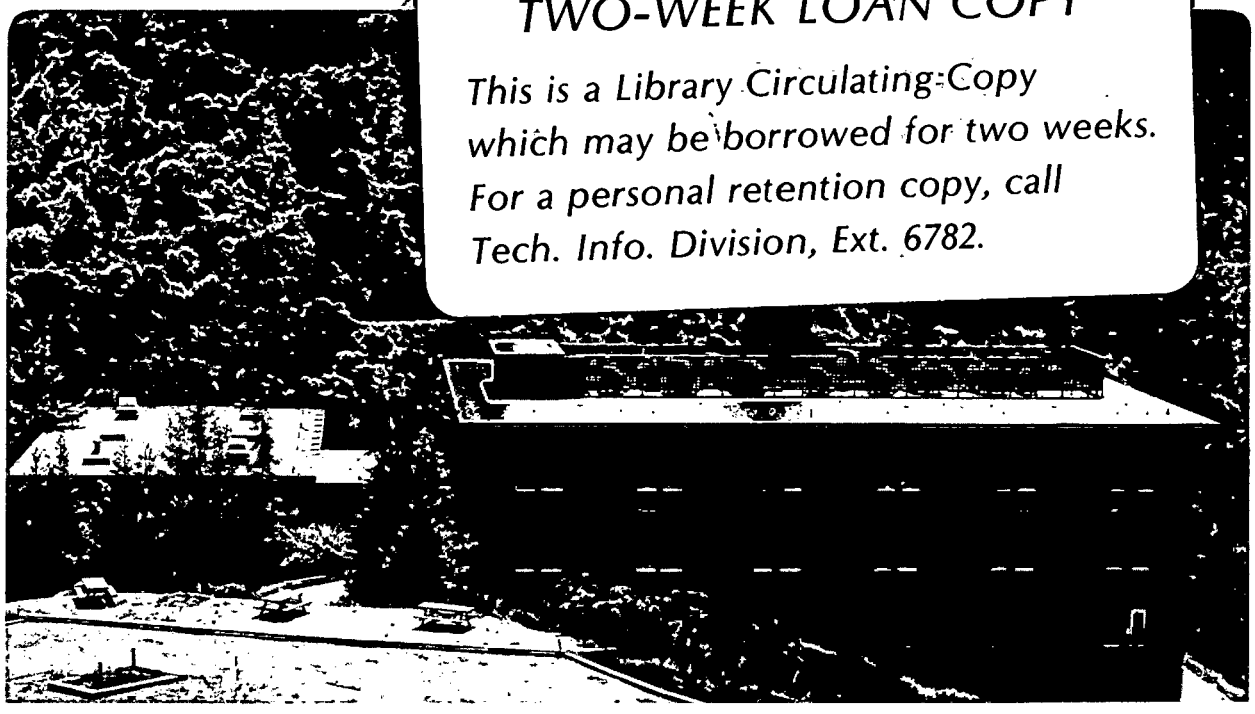

Prepared for the U.S. Department of Energy under Contract DE-AC03-76SF00098

DISCLAIMER

LBL-15540

CORE-LEVEL PHOTOELECTRON AND AUGER SHAPE-RESONANCE PHENOMENA IN CO, CO_2, CF_4, AND OCS

C. M. Truesdale,* D. W. Lindle, P. H. Kobrin,† U. E. Becker,‡
H. G. Kerkhoff,‡ P. A. Heimann, T. A. Ferrett, and D.A Shirley

Materials and Molecular Research Division
Lawrence Berkeley Laboratory
and
Department of Chemistry
University of California
Berkeley, California 94720

Cross sections and angular-distribution asymmetry parameters were measured directly for C(KVV) Auger electrons and C 1s photoelectrons from CO, CO_2, CF_4 and OCS, O(KVV) Auger electrons and O 1s photoelectrons from CO and CO_2, and S(LVV) Auger electrons and S 2p photoelectrons from OCS using synchrotron radiation. The measurements were made in the photon-energy ranges 270-350 eV, 545-680 eV and 160-190 eV, respectively. Shape resonances were observed in all of these molecular systems. The cross-section results are compared with previous experimental data obtained by electron energy-loss measurements, electron-ion coincidence results and photoabsorption studies. The asymmetry-parameter results are the first of their kind for these molecular core levels. The present results are compared with available theoretical predictions obtained from Stieltjes-Tchebycheff imaging techniques, Hartree-Fock static-exchange calculations, and the multiple-scattering method.

*Present address: Research and Development Division, Corning Glass Works, Corning, NY 14831.
†Present address: Department of Chemistry, Pennsylvania State University, University Park, PA 16802.
‡Permanent address: Technische Universität Berlin, Fachbereich Physik, 1000 Berlin 12, West Germany.

I. Introduction

Direct photoexcitation of molecular core levels by variable-energy synchrotron radiation yields photoelectrons and Auger electrons. The differential cross section for ejecting electrons by linearly polarized light varies as

$$\frac{d\sigma(h\nu,\theta)}{d\Omega} = \frac{\sigma(h\nu)}{4\pi}\left[\, 1 + \beta(h\nu)P_2(\cos\theta)\,\right] , \qquad (1)$$

provided that the initial photoionization mechanism has electric-dipole character and that the initial system is randomly oriented.[1] Here $P_2(\cos\theta)$ is the second Legendre polynomial, θ is the angle between the polarization direction of the exciting light and the electron propagation direction, and $h\nu$ is the photon energy. For photoelectrons, the kinetic energy ϵ of a peak corresponding to a given orbital of binding energy E_B is given by $\epsilon = h\nu - E_B$. For Auger electrons, the kinetic energy of a given channel is invariant with photon energy (post-collision interaction is negligible in this work). In both cases, a complete description of the differential cross section can be given by the two functions $\sigma(h\nu)$ and $\beta(h\nu)$, the cross section and asymmetry parameter, respectively. They in turn can be determined by measuring $d\sigma(h\nu,\theta)/d\Omega$ at two known angles θ. Given the close relationship between $h\nu$ and ϵ, these parameters are often listed as $\sigma(\epsilon)$ and $\beta(\epsilon)$ for photoelectrons. The notations $\sigma_A(h\nu)$ and $\beta_A(h\nu)$ are used here to denote the properties of Auger

transitions, and in particular for this work, they represent properties averaged over all of the Auger peaks produced by the decay of a vacancy in a given subshell. In addition, Dill et al.[2] have used the notation $\beta_m(h\nu)$ to denote the alignment in the initial state of an Auger transition. The asymmetry parameter of each Auger transition is given by

$$\beta_A(h\nu) = \beta_m(h\nu)A \quad , \tag{2}$$

where $\beta_m(h\nu)$ is the orientation parameter and A is a photon-energy independent quantity specific to each Auger-decay process.

For photon energies near the core-level binding energies of electrons in molecules, resonances in cross sections and asymmetry parameters may exist. A certain class of these resonances is associated with the trapping of the outgoing photoelectron in a quasi-bound state by the molecular potential. These are termed "shape resonances", and are expected to constitute sensitive probes of the molecular potential. Although shape resonances for core-electron excitation in molecules have been the subject of extensive theoretical investigation, notably by Dill et al.,[2] they have not to our knowledge been observed in a direct photoionization experiment; an experiment in which both the energy and direction of tne incoming photon and the outgoing electron are defined. In this paper, and in an earlier preliminary report on CO,[3] we describe the first direct gas-phase measurements of molecular core-level shape resonances in the

photoelectron cross section $\sigma(\varepsilon)$ and Auger electron cross section $\sigma_A(h\nu)$, and the first measurements of any kind on the photoelectron asymmetry $\beta(\varepsilon)$ and Auger electron asymmetry $\beta_A(h\nu)$ of these same transitions.

Our results can be compared with related work in several cases. Experimentally, these include photoabsorption,[4,5] electron energy loss,[6-12] electron-ion coincidence,[13] Auger yield,[14] and valence-orbital photoemission.[15] Several theoretical predictions are available in addition to the multiple-scattering method (MSM) $X\alpha$ results.[2] The Stieltjes-Tchebycheff moment theory (STMT) constructs ground-state wavefunctions of Hartree-Fock quality from which static-exchange potentials are approximated to account for the nonlocal properties of the core-hole states. Pseudospectra are then produced that account for the frequencies and oscillator strengths of various transitions to discrete valence and continuum valence-like orbital channels. Padial et al.[16-17] have used the STMT formalism to calculate the partial cross sections for C 1s and O 1s photoemission from CO and CO_2. Recently, a Hartree-Fock static-exchange calculation by Lucchese and McKoy[18] has yielded C 1s and O 1s cross sections and asymmetry parameters for CO_2.

There are six sections to follow. The experiment is described in the next section. The results and discussion for CO, CO_2, CF_4, and OCS will be presented in Sections III-VI, respectively, and conclusions will be presented in Section VII.

II. Experimental

The experimental apparatus has been described previously.[19] Briefly, gaseous samples were excited by photons from the grazing-incidence "grasshopper" monochromator on Beam Line III-1 at the Stanford Synchrotron Radiation Laboratory.[20] The monochromator was operated with a 1200 ℓ/mm holographically-ruled grating. Our double-angle time-of-flight (TOF) spectrometer detected the ejected electrons at 0° and 54.7° relative to the photon polarization axis. Relative cross sections were determined from the electron intensities measured with the 54.7° detector, and the asymmetry parameters were derived from the ratio of intensities measured at 0° and 54.7°.

Most spectra were collected for 1000 sec, the exceptions being those of the S 2p photoelectron and S(LVV) Auger peaks of OCS, which were collected for 300 sec. In the CO, CO_2, CF_4, and OCS carbon and oxygen K-shell experiments, an aluminum window (1500Å thickness) isolated our chamber from the ultra-high vacuum monochromator. A vitreous carbon window (1000Å thickness) was used for the OCS sulfur L-shell experiments.

Cross sections and asymmetry parameters were corrected in a calibration procedure described in Ref. 21. The asymmetry parameters are corrected for the relative efficiency of the two detectors as a function of the kinetic energy of detected electrons. Comparisons are made between accepted literature values for the asymmetry parameters of Ne 2s and 2p photoelectrons for photon energies of 50-300 eV[22]

and the ratio of their measured intensities at 0° and 54.7°. A small (up to several percent) unpolarized component of the synchrotron radiation and any small misalignment of the photon beam with respect to the analyzers is thereby corrected for in the final determination of unknown asymmetry parameters.[21] Likewise, our measured relative cross sections have been corrected for the (energy-dependent) transmission characteristics of the 54.7° detector by comparison with the partial cross sections of the Ne 2s and 2p photoionization channels.[22]

Excitation spectra of discrete subthreshold resonances (e.g., $\sigma \rightarrow \pi^*$ for CO, CO_2, and OCS, and $\sigma \rightarrow 3sa_1$ for CF_4) were used to calibrate the monochromator energy scale. (The π^* notation refers to the excitation of the core carbon and oxygen electrons to the first π unoccupied bound molecular orbital.) The monochromator bandpass was determined by the observed widths of these resonances. The CO C 1s measurements were done with monochromator bandpasses of 0.5 and 2 eV FWHM. The 0.5 eV resolution measurements were performed in the region of the $\sigma \rightarrow \pi^*$ discrete transition. For the CO_2 C 1s measurements a 2 eV bandpass was used throughout. The S 2p and S(LVV) Auger experiments on OCS used a monochromator resolution of 1 eV, while the OCS C 1s studies used a bandpass of 4 eV. The O 1s measurements performed with first-order light for CO were carried out with a monochromator bandpass of 5 eV, and the second-order O 1s measurements for CO and CO_2 were performed with 4 eV monochromator resolution. In each case an additional 3% of the kinetic energy of the electrons

(arising from the geometry of our spectrometer) must be factored in to account for the overall resolution of the peaks in our spectra. For some spectra, the electrons were retarded for 16.9 cm of the total 28.5 cm flight path by means of retarding cages inside the flight tubes of the TOF detectors. The resolution of photoelectron and Auger peaks was significantly improved by this procedure.

At certain photon energies, peaks appeared in the TOF spectra that were produced by a second-order (i.e. $2h\nu$) component of the photon beam. In principal, the second-order contribution could cause errors in the measured photoelectron cross sections because the normalization to the photon flux would not accurately represent the first-order photon flux which produced the photoelectron peak. Smaller errors related to the second-order component could also afflict the Auger cross sections and asymmetry parameters. All of these effects are significant only if the second-order contribution changes as a function of energy. No second-order light corrections for the cross-section data and the Auger asymmetry-parameter data were made, however. For the C 1s measurements of CO and CO_2, the incident photon flux experienced only a small drop at the C K-edge, precluding any large changes in the second-order light contribution to these experiments. This was not true for the CF_4 and OCS C 1s experiments, in which the drop was several times larger. In any case, because of the small observed intensity for the second-order C 1s photoelectron peak in all of our spectra, and because of the general agreement between our cross-section data and previous measurements,

second-order corrections are probably not substantial. It should be noted that second-order contributions will have no effect on the measurements of photoelectron asymmetry parameters.

Spectra taken with first-order photon energies near the C 1s, O 1s and S 2p thresholds in general contained valence-orbital photoelectron peaks that overlapped with, and were unresolvable from, the Auger peaks. However, extrapolation from spectra taken with photon energies too low to excite the discrete resonances below these thresholds enabled us to estimate the effects of the valence photoelectrons on the Auger data. Attempts to remove these valence contributions have been made where possible. However, it is to be kept in mind that significant 'valence effects' may still be included in all of the Auger cross sections $\sigma_A(h\nu)$ and asymmetry parameters $\beta_A(h\nu)$ presented here. These effects are manifested as an additive (energy-independent) constant to $\sigma_A(h\nu)$, causing little or no effect on the qualitative results. For $\beta_A(h\nu)$, however, the measured asymmetry parameter is a weighted average of the Auger asymmetry parameter and the valence asymmetry parameter, thus valence contributions will cause stronger effects for lower Auger yields. In all cases, the uncorrected $\beta_A(h\nu)$ tended to higher values because of the valence contribution. In most cases, the qualitative results presented for $\beta_A(h\nu)$ do not depend on the accuracy of the correction. The implications of the valence corrections will be addressed for particular instances in which the results are seriously affected.

III. CO Results and Discussion

Some of the CO shape-resonance results reported here were presented and discussed in an earlier report.[3] We include them here for completeness, but refer the reader to that report for its complementary discussion.

The ground-state electronic configuration of CO is $1\sigma^2 2\sigma^2 3\sigma^2 4\sigma^2 1\pi^4 5\sigma^2 \quad {}^1\Sigma^+$. The 1σ orbital is basically O 1s-like (E_B = 541.2 eV), the 2σ is C 1s-like (E_B = 295.9 eV[23]), and the other four orbitals constitute the valence shells.

Two TOF spectra of CO, converted to kinetic-energy scales, are shown in Figs. 1 and 2. The spectrum in Fig. 1 was collected with a retarding voltage of 150 volts. The $5\sigma^{-1}$, $1\pi^{-1}$, and $4\sigma^{-1}$ photoelectron peaks, with binding energies of 14.9, 17.6, and 20.5 eV, respectively, are unresolved, but the $3\sigma^{-1}$ peak, with a binding energy of 35.4 eV, is distinct. Peaks corresponding to the C(KVV) and O(KVV) Auger electrons, and the C 1s (from 2nd order light) and O 1s (from 3rd order light) photoelectrons are also observed. A spectrum taken with a retarding potential of 5 volts is shown in Fig. 2. The C 1s (first order) and O 1s (second order) photoelectron peaks are evident, and the identities of the other features can be inferred from Fig. 1.

We note that the C(KVV) Auger peaks have kinetic energies of 220 to 273 eV. Using the notation of Moddeman et al.,[24] the B-1 peak ($5\sigma^{-1}1\pi^{-1}$ final state) with a kinetic energy of ~255 eV is

convoluted with B-3 ($5\sigma^{-2}$) and the weak B-2 ($4\sigma^{-1}5\sigma^{-1}$) Auger band.[25,26] Other Auger transitions observed by Moddeman et al. are present also (B-6 to B-10 are grouped together into the peak labeled B). The bands labeled by Moddeman et al. as A-1 to A-11 (autoionization) can only be produced by excitation of a 2σ electron to a Rydberg state below the C 1s threshold (such as $\sigma \rightarrow \pi^*$), and thus are not observed in Figs. 1 and 2. The oxygen Auger peaks have kinetic energies of 413 to 517 eV. The largest O(KVV) peaks have been identified as the B-5 ($1\pi^{-2}$) and B-7 ($4\sigma^{-1}1\pi^{-1}$) bands.[25] Our peak at a kinetic energy of 495 eV corresponds to B-5 convoluted with B-7 (shake-up) and B-4, and the shoulder at about 500 eV is the B-1 band ($5\sigma^{-1}1\pi^{-1}$).[25] The results of ab-initio molecular Auger calculations by Ågren[26] suggest that the large C(KVV) Auger peaks arise from vacancies in the 5σ orbital, and that vacancies in the 3σ, 4σ, and 1π orbitals dominate the O(KVV) Auger spectrum.

The cross section $\sigma_A(h\nu)$ and asymmetry parameter $\beta_A(h\nu)$ averaged over all of the C(KVV) Auger transitons in CO are shown in Fig. 3. The cross section $\sigma_A(h\nu)$ for the $2\sigma \rightarrow 2\pi(\pi^*)$ resonance, at 287.3 eV photon energy,[6,7,12,13] has been scaled to the absolute oscillator strength for this resonance reported by Tronc et al.[6] This discrete resonance is over an order of magnitude more intense than the continuum excitations above the C 1s threshold. For photon energies above the discrete resonance, the C(KVV) curve was scaled by a constant factor to agree with the C 1s photoelectron cross section at 315 eV, which was normalized in turn to the electron-ion

coincidence measurements,[13] shown by the dashed curve in Fig. 3. The continuum region shows structure arising from the C 1s photoelectron shape resonance. In normalizing the Auger yield to the C 1s cross section we have assumed a negligible fluorescence yield.

The asymmetry parameter for the C(KVV) channel in CO after removal of valence contributions is nearly zero over the entire region where measurements were taken. The implications of this are discussed in the previous report.[3] The conclusions made there are generally applicable to all of the $\beta_A(h\nu)$ results reported in this paper. Near 295 eV, $\beta_A(h\nu)$ deviates from the near-zero value measured at other energies. The published electron-energy loss measurements[12] show complex structure near this energy. Our data indicate that in this region the excited CO molecule is oriented and yields an asymmetry in the C(KVV) Auger channel. No further interpretation is warranted, because the nature of the discrete resonance at 295 eV is not well established.

Turning now to the 287.3 eV resonance, the orientation parameter for the excited state following the $\sigma \rightarrow \pi^*$ transition is predicted to have a value of -1.[2] This prediction has essentially been confirmed by Stohr et al.[14] for CO adsorbed and oriented on a surface. It seems inescapable that CO^* is strongly oriented in the π-resonance excited state. There are two possible ways to reconcile this orientation with our observation that the kinetic-energy integrated C(KVV) asymmetry parameter is essentially zero at 287.3 eV. First, the A_j factors for the various Auger transitions of

fractional strength f_j could have values that average the measured Auger asymmetry parameter $\beta_A(h\nu)$ to zero, according to

$$\beta_A(h\nu) = \beta_m(h\nu) \sum_j A_j f_j(h\nu) \qquad \left(\frac{-1}{2} \leq A_j \leq 1 \right) . \tag{3}$$

This can also explain the discrepancy between the calculated orientation parameter $\beta_m(h\nu)$,[2] shown in Fig. 3, and our asymmetry-parameter values for the C(KVV) channel above the C 1s threshold. Well-resolved Auger spectra will have to be recorded to test this possibility. Our own attempts to obtain such spectra will be described below, after we address the alternative explanation for a near-zero asymmetry parameter.

The above idea that $\beta_A(h\nu)$ is near zero because of cancellation of asymmetries is difficult to accept, especially if it must be invoked twice; i.e., for the π resonance and again for the continuum states. An attractive alternative explanation for the near-zero β of the π resonance is the "spectator" model, in which the excited electron retains the total orientation of the system in a π^* orbital, while the subsequent Auger electrons show only an isotropic distribution, as required by angular-momentum conservation. The molecular "core" would then behave somewhat like an atom with a K-shell hole and exhibit no asymmetry in its Auger decay. A similar result has been obtained for Ne(KLL) Auger electrons after 1s → 3p excitation.[27]

In an attempt to test the first explanation, we used selected

retarding potentials to study the kinetic-energy distribution of the Auger electrons for photon energies above and below the C 1s threshold. Two typical spectra, excited by photons on resonance at 287.3 eV and above threshold at 296.8 eV, are shown in Fig. 4. The large C(KVV) peak at 265 eV kinetic energy in the 287.3 eV spectrum corresponds to the B-1 band ($5\sigma^{-1}1\pi^{-1}$) in the 296.8 eV spectrum. The shoulder at lower energy contains other C(KVV) Auger lines (see Fig. 1). The B-1 peak in the below-threshold spectrum has a kinetic energy ~13 eV higher than its counterpart in the above-threshold spectrum because the initially excited electron is still present. High-resolution electron-electron coincidence measurements of C(KVV) Auger spectra for CO[28] and comparable measurements of N(KVV) Auger spectra for N_2[29] have shown a similar shift. Because of the low resolution of our spectra, we could only confirm that the mean energies and overall shapes of the spectra were different. We could not establish whether or not the asymmetry parameter varies with kinetic energy across a spectrum.

The cross section and asymmetry parameter of the peak which includes the unresolved X, A, and B states of CO^+ derived by ionization of 5σ, 1π, and 4σ electrons, and the C 1s peak in second order, also were derived from our data. The cross section showed little variation with photon energy in the range 270-315 eV, and β was between 1.5 and 2.0. The data showed scatter because of the difficulty of deconvoluting these peaks from the Auger structure, but their overall behavior assured us that the curves derived for the

Auger peaks accurately represent the effects on the Auger channels.

The results for the C 1s photoelectron channel are presented in Fig 5. Our relative cross sections were scaled to the electron-ion coincidence measurements of Kay et al.,[13] shown by the open circles. The C 1s cross section shows a weak shape-resonance maximum centered around 307 eV, in good agreement with the results of Kay et al. and with predictions of an STMT calculation (solid curve).[16] In the STMT work two major subchannel excitations were invoked to describe the 2σ K-shell excitations. Those were the $2\sigma \rightarrow k\sigma$ and the $2\sigma \rightarrow k\pi$ continuum transitions. The $\ell=3$ partial wave in the $\sigma \rightarrow k\sigma(\epsilon f)$ transition has been suggested as being responsible for the σ shape resonance.[30-33] Also shown in Fig. 5 is a dashed curve representing the MSMXα calculation.[33] This curve shows a maximum at the right energy, but its width is narrower than the experimental value, and its contrast ratio is about twice the experimental result.

The asymmetry parameter for C 1s photoionization confirms the existence of a shape resonance with a weak minimum at 303 eV. The variation of the measured $\beta(\epsilon)$ falls between the predictions of the localized-hole MSMXα calculations of Dill et al.[32] and Grimm,[34] shown by the solid curve and dashed curve, respectively. The overall shapes of the calculated $\beta(\epsilon)$ curves are in very good agreement with the present results, except for predicting a contrast ratio larger than observed.

The C 1s (2nd order) peak could be deconvoluted in our spectra for photon energies of 308 to 314 eV; i.e., for second-order photon

energies ranging from 616 to 628 eV. In those spectra, $\beta(\varepsilon)$ was determined to have a mean value of 2.0(1). Of course, $\beta = 2$ is expected for an atomic $ns \rightarrow \varepsilon p$ transition. In the high kinetic-energy regime it may be plausible to consider the C 1s excitations in molecular CO as atomic excitations because the scattering dynamics should not include resonances, and the outgoing electron has little interaction with the molecular potential.

The O(KVV) Auger results are displayed in Fig. 6. The data are incomplete because the oxygen edge was a secondary objective of this study, as a consequence of the poor performance of the monochromator in this energy range. Our results were derived by using both first-order and second-order light. No data were taken below 540 eV in either order, and the range 550-570 eV was largely missed, thereby precluding a definitive study of shape-resonance phenomena. The results are nonetheless of some interest.

The O(KVV) cross section closely mimics the O 1s cross section (to be discussed later), as expected. Both the cross-section and asymmetry-parameter results were easily determined because the peak fell at a high kinetic energy and was well separated from other features. For $h\nu$ = 560-630 eV, the asymmetry-parameter data lie in the range $-0.1 \leq \beta \leq 0.3$ with no real trends, and a horizontal straight line fits the data within their statistical accuracy, yielding a value of 0.10(2).

Our six points near threshold, in the range $h\nu$ = 545-555 eV, show a larger β in the range 0.3-0.5. It is possible that these points

provide the first evidence for a shape-resonance effect on an Auger asymmetry parameter, as predicted by Dill et al.[2] Their calculated curve for the orientation parameter β_m is shown in Fig. 6. Clearly more work is needed on this question.

The results for the O 1s photoelectron peak are presented in Fig. 7. There is general agreement among our cross-section data, the photoabsorption measurements,[4] and the STMT calculation of Padial et al.[16] Our measurements based on first-order and second-order light were scaled separately to the photoabsorption data at 545 and 562 eV, respectively. The O 1s cross section clearly shows a shape resonance near 550 eV.

The dearth of measurements between 550 and 570 eV prevents the determination of the existence of a minimum in the O 1s asymmetry parameter predicted by the localized-hole MSMXα calculations of Grimm[34] and Dill et al.[32] We find that $\beta(\epsilon)$ increases rapidly from 0.7 at 545 eV toward an asymptotic value above 1.5 by 570 eV. Whether there is more structure in the 550-570 eV range is unknown. At higher energies our data appear to approach an asymptotic value of 1.6(1). The MSMXα calculations[32,34] show good agreement with this result, approaching an asymptote at this level or higher. Similar behavior was observed both experimentally and theoretically for the C 1s shell (see Fig. 5).

Shake-up structure was observed near the O 1s peak. A TOF spectrum taken with second-order light at 630 eV, converted to an energy scale, is shown in Fig. 8. The structure is probably the

result of the $1\pi \rightarrow 2\pi$ shake-up transition. We find that this structure has an intensity that is 13(3)% of the O 1s main-line intensity. Carlson et al.[35] reported that this state has ~10% of the O 1s intensity. Aarons et al.[36] performed an unrestricted Hartree-Fock calculation to assign shake-up thresholds and intensities in the high-energy limit. They predicted that the $1\pi \rightarrow 2\pi$ shake-up peak lies 16 eV above the O 1s peak and should have 15.4% of the O 1s intensity. The agreement between their calculation and our measurement is good.

IV. CO_2 Results and Discussion

The ground-state electronic configuration of CO_2 can be written $1\sigma_g^2 1\sigma_u^2 2\sigma_g^2 3\sigma_g^2 2\sigma_u^2 4\sigma_g^2 3\sigma_u^2 1\pi_u^4 1\pi_g^4 \ ^1\Sigma_g^+$. The $1\sigma_g$ and $1\sigma_u$ orbitals (unresolved in this work) are linear combinations of atomic O 1s orbitals with an average binding energy of 541.2 eV. The $2\sigma_g$ orbital is basically a C 1s atomic orbital with a binding energy of 297.5 eV. The remaining molecular orbitals have binding energies below 50 eV and were not studied in this work. A spectrum is shown in Fig. 9, where the various peaks have been identified. The dominant C(KVV) peaks have been assigned as having mainly $1\pi_u^{-2}$ and $4\sigma_g^{-1}1\pi_g^{-1}$ final states.[26] Some of the O(KVV) peaks of CO_2 still do not have unambiguous assignments, but the $1\pi_g^{-2}$-hole states probably account for most of the high kinetic-energy Auger peaks.[26]

In Fig. 10, the CO_2 C(KVV) Auger cross section $\sigma_A(h\nu)$ shows a discrete resonance transition $[2\sigma_g \rightarrow 2\pi_u(\pi^*)]$ centered near 290 eV and a broad shape resonance $[2\sigma_g \rightarrow 4\sigma_u(\sigma^*)]$ with a maximum near 310 eV. The C(KVV) Auger cross-section results were scaled at 315 eV to the C 1s partial cross section derived from the electron-energy loss studies of Wight and Brion,[9] which were themselves scaled to agree with the STMT calculations of Padial et al.[17] at 300 eV.

The results for the CO_2 C(KVV) asymmetry parameter are also presented in Fig. 10. At the $2\pi_u(\pi^*)$ resonance, $\beta_A(h\nu)$ is small

but apparently nonzero, similar to the result for the C(KVV) channel of CO at the $2\pi(\pi^*)$ resonance. The remainder of the asymmetry-parameter results must be interpreted cautiously. The highest values of $\beta_A(h\nu)$ fall at energies for which the Auger peak intensity is very weak; i.e., $h\nu$ = 296, 300, and $h\nu > 330$ eV, and cannot be interpreted with any confidence. In the range $300 \leq h\nu \leq 325$ eV, $\beta_A(h\nu)$ shows scatter well outside of statistics, but appears to be slightly positive (as for CO). The discussion given for the CO C(KVV) Auger asymmetry is also appropriate for CO_2.

The results for the C 1s photoelectron channel are presented in Fig. 11. The cross section for the C 1s peak of CO_2 was scaled in the same way as the C(KVV) cross section. The σ shape resonance peaking at 311 eV is more evident than in CO. Both of the theoretical models (HF static exchange and MSMXα) are fairly accurate in determining the shape of the peak in the cross section, but the energy of the broad shape resonance is calculated to lie 5-6 eV closer to threshold; at ~8 eV rather than the experimental value of 14 eV kinetic energy. Grimm has suggested that the C 1s shape resonance is attributable to the ℓ=2,3 channels in the $2\sigma_g \rightarrow 4\sigma_u(\sigma^*)$ continuum transition. Wight and Brion[9] suggested that the structure present at 303 eV is attributable to $1\pi_u$ shake-up ($1\pi_u \rightarrow 2\pi_u$). Both theories miss this structure because they do not include two-electron excitations.

The effect on the asymmetry parameter of the C 1s peak in CO_2 is also more dramatic than in CO, appearing as a broad minimum

centered around 318 eV. The HF static-exchange calculation[18] is in better agreement in predicting the overall shape of $\beta(\varepsilon)$ than the unlocalized-hole MSMXσ calculation.[34] Nonetheless, the unlocalized-hole MSMXα predicts the energy position for the shape-resonance minimum very close to our measurements. The localized-hole MSMXα calculation of $\beta(\varepsilon)$ for the C 1s channel[34] predicts the shape resonance too close to threshold.

The O(KVV) results are presented in Fig. 12. The cross section of the O(KVV) channel should be nearly equal to the O 1s partial cross section when the photon energy is above the O 1s threshold. Thus, we shall use the Auger yield $\sigma_A(h\nu)$ for the O(KVV) channel of CO_2 to make comparisons to previous O 1s cross-section measurements and theoretical calculations. The partial cross section for the CO_2 O(KVV) channels was scaled to the O 1s photoabsorption measurements of Barrus et al.[4] at 555 eV to yield absolute partial cross sections. The Auger yield for the O(KVV) peak is then in excellent agreement with the photoabsorption measurements as a function of energy. Both theoretical curves predict the energy of the O 1s shape resonance to be near 560 eV, but the STMT calculation[17] is in closer quantitative agreement with the experiment in predicting the shape of the cross section. Barrus et al. stated that they observed weak structure at ~580 eV in their absorption curve, which was proposed to be related to shake-up structure. We see similar structure in our yield data.

The measured O(KVV) asymmetry parameter, shown in Fig. 12, starts at a value near 0.25 at 550 eV, decreases to 0.1 at 575 eV, has a weak

maximum near 580 eV, and remains close to 0.1 from 600 eV to 680 eV. The possible structure near 580 eV corresponds to the same feature observed in $\sigma_A(h\nu)$, and may be a result of autoionization.

The asymmetry parameter $\beta(\varepsilon)$ for the O 1s channel is shown in Fig. 13. It rises from 0.8 at ~550 eV to ~1.5 by 565 eV, and remains near this value up to 680 eV. Our results are sparse at the low energies [the region where both the HF static-exchange and the localized-hole MSMXα calculations predict minima in $\beta(\varepsilon)$], and the monochromator resolution was poor in this region. Therefore, we cannot infer anything about a possible minimum for the asymmetry parameter.

After expanding the spectra around the O 1s peak, O 1s satellite structure was observed. In Fig. 14, we present a TOF spectrum collected with second-order light at an energy of 630 eV. The largest O 1s shake-up peak is located at about 19 eV above the O 1s threshold. Allan et al.[37] have attempted to assign the total O 1s shake-up structure of CO_2. They suggest that two shake-up peaks at 13.8 eV and 16.0 eV (referenced to the O 1s main peak) arise from transitions involving the excitations $4\sigma_g \rightarrow 5\sigma_g$ (14.5 eV), $1\pi_u \rightarrow 2\pi_u$ (15.2 eV), and $3\sigma_u \rightarrow 4\sigma_u$ (15.5 eV). The branching ratio for the total O 1s shake-up intensity to the O 1s main-line intensity is tabulated in Table I. Theoretical calculations[36] have indicated that ~20% of the intensity of the O 1s main line is present in the O 1s satellite structure. The average value from this work for the branching ratio of the satellite peaks from 11 to 28 eV above the

O 1s binding energy and for photon energies between 592 and 632 eV is 21(3)%. Allan et al.[37] found that when CO_2 was excited by Mg Kα radiation (1254.6 eV), the sum of the O 1s shake-up peaks was 17.5% of the intensity of the O 1s photoelectron peak.

V. CF_4 Results and Discussion

The ground-state electronic configuration of this tetrahedral molecule can be written $1t_2^6 1a_1^2 2a_1^2 3a_1^2 2t_2^6 4a_1^2 3t_2^6 1e^4 4t_2^6 1t_1^6 \ ^1A_1$.[38] The $1t_2$ and $1a_1$ molecular orbitals are described by a linear combination of F 1s atomic orbitals. The $2a_1$ molecular orbital is formed almost entirely from a C 1s atomic orbital and has a binding energy of 301.8 eV. A TOF spectrum of CF_4 at 318.8 eV photon energy is shown in Fig. 15. The features present are the C 1s peak, the C(KVV) Auger peak, the valence photoionization channels, and the F(KVV) Auger peaks which arise from third-order light. We shall discuss only the C 1s and C(KVV) peaks, which were observed in spectra taken at photon energies between 280 and 350 eV.

The derived parameters for the C(KVV) and C 1s peaks of CF_4 are plotted in Figs. 16 and 17. In these figures, our derived partial cross sections are compared to the electron-energy loss measurements of Wight and Brion[10] and the photoabsorption results of Bachrach et al.[5] There are no theoretical or other experimental $\beta(\epsilon)$ results for the C 1s and C(KVV) channels of CF_4.

The measured C(KVV) Auger cross section $\sigma_A(h\nu)$ was scaled to the results of Bachrach et al.[5] at 302 eV. The discrete resonance at 298 eV has been assigned as arising mostly from the $2a_1 \rightarrow 3sa_1$ Rydberg-type excitation, with small contributions from 3p and 3d Rydberg orbitals.[10] To account for valence contributions to their results, their measured cross section below the discrete resonance

energy was assumed to be composed entirely of valence photoelectrons and was therefore subtracted prior to scaling our results. There is good agreement between the photoabsorption study and the present work. Differences observed between the two could be a result of our using a 4 eV bandpass, or of the uncertainty of the first-order photon flux for the monochromator at the carbon K-edge as discussed in Sect. II. The intensity ratio of the discrete resonance to the continuum σ shape resonance in CF_4 lies between those observed in CO and CO_2.

The C(KVV) Auger asymmetry parameter for CF_4 is also shown in Fig. 16. The value of $\beta_A(h\nu)$ at the discrete resonance is near zero, as was the case for the C(KVV) peaks in CO and CO_2. The value of $\beta_A(h\nu)$ for photon energies above the C 1s threshold in CF_4 lies in the range 0.2-0.3. It shows no variation in the continuum shape-resonance region around 315 eV. Because the $3a_1$ and $2t_2$ molecular orbitals are inextricably convoluted in our "Auger" peak, we are inclined tentatively to conclude that the nonzero value of the observed asymmetry of this peak may be largely ascribed to contributions from these orbitals.

The C 1s relative cross section in Fig. 17 was scaled in a fashion similar to the C(KVV) yield, but at 310 eV. The cross section exhibits a broad shape resonance centered at approximately 315 eV. The width of the resonance agrees with the electron-energy loss measurements.[10]

The C 1s asymmetry parameter in Fig. 17 starts at a value of ~0.7 at 306 eV, exhibits a broad minimum with a value of about 0.3,

steadily increases, and remains above 1.0 from 330 eV to 350 eV. The width of the minimum falls between the CO and CO_2 C 1s results, and follows the ordering CO < CF_4 < CO_2. This ordering also applies to the C 1s molecular shape-resonance contrast ratio. Theoretical studies of the C 1s cross section and asymmetry parameter in CF_4 are needed. These experimental results appear to be useful in qualitatively describing the systematics of shape-resonance phenomena.

VI. OCS Results and Discussion

The ground-state electronic configuration of OCS can be written $1\sigma^2 2\sigma^2 3\sigma^2 4\sigma^2 5\sigma^2 1\pi^4 6\sigma^2 7\sigma^2 8\sigma^2 9\sigma^2 2\pi^4 3\pi^4$, $^1\sum^+$. We present angle-resolved studies of the 3σ, 5σ and 1π orbitals, which correspond, respectively, to the C 1s shell with a binding energy of 295.2 eV, and the sulfur $L_{2,3}$ doublet, with edges at 170.6 and 171.6 eV. We have not attempted to resolve the two sulfur photoelectron peaks, and will adopt an average ionization threshold of 171 eV for this subshell, which we henceforth denote as S 2p. The carbon K-shell studies will be presented first, followed by the S 2p and the S(LVV) results. Spectra of OCS can be found in Figs. 18 and 19.

The C(KVV) results are shown in Fig. 20. The $3\sigma \rightarrow 4\pi(\pi^*)$ discrete resonances have been observed in electron-energy loss measurements,[11] where the largest is centered at 288 eV. Wight and Brion[11] have also observed discrete structure in the continuum range. Grimm[34] has predicted that the excitations of the C 1s electron into the continuum would show two shape resonances; both the ℓ=3,4 partial waves of the σ channel are expected to have delayed onsets. We therefore sought evidence to test this prediction.

The OCS C(KVV) Auger cross section shows a large discrete transition below the C 1s threshold. Above threshold there is convincing evidence for only one maximum in the cross section near 312 eV. The electron-energy loss measurements,[11] which correspond to the solid curve, have been scaled to our data at 291.2 eV. The

valence intensity is apparent in the measurements below 285 eV photon energy. No attempt was made to deconvolute it from the Auger results because of large uncertainties introduced for this case. The results of Wight and Brion show a much smaller intensity for energies above the carbon K edge than do the present data. We offer no explanation for this discrepancy.

The C(KVV) Auger asymmetry parameter $\beta_A(h\nu)$ is presented in the bottom panel of Fig. 20. Again $\beta_A(h\nu)$ is nearly zero at the discrete π^* resonance, as was true for all the other molecules. The value of $\beta_A(h\nu)$ generally is between -0.2 and zero through the entire energy range, although there is an increase near the C 1s threshold. A broad minimum is present in the asymmetry parameter near 315 eV. These features are probably consequences of valence contributions under the Auger peaks.

The C 1s cross section $\sigma(\epsilon)$, shown in Fig. 21, may have two maxima near 305 eV and 312 eV. If the first and second maxima are indeed the f and g partial-wave shape resonances, respectively, then the g-wave experiences a stronger resonance.

In the bottom panel of Fig. 21, the C 1s asymmetry-parameter data are shown. The localized-hole MSMXα results of Grimm[34] are represented by the solid curve. From our earlier results on CO and CO_2, the $\beta(\epsilon)$ values calculated with the localized-hole potential model are expected to show better agreement with our measurements than the unlocalized-hole MSMXα calculation (not shown), and indeed this is the case. Although scatter is present in the data, it is clear that

the localized-hole MSMXα calculation predicts the two minima observed, but at slightly lower energies.

The sulfur 2p shell has been studied previously in the region of the sulfur L edges by optical absorption[39,40] and electron-energy loss methods.[11] Our work is the first photoemission investigation of the sulfur 2p shell of OCS in this energy range. We shall present results for the S 2p and the S(LVV) channels. The S 2p shell of OCS closely resembles the S 2p shell in atomic sulfur. Deviations from atomic theoretical predictions might therefore highlight molecular effects in S 2p photoemission. The S(LVV) results will complement and test these interpretations.

The S 2p photoemission measurements were performed over the photon energy range 160-190 eV. The data are presented in Figs. 22 and 23, along with the electron-energy loss results.[11] We have scaled the electron-energy loss data to our data to give the best agreement.

There is excellent agreement between the electron-energy loss measurements and the relatively sparse data for the S(LVV) Auger channel shown in Fig. 22. The discrete resonances are associated with the excitation of the S 2p electron to the $4\pi(\pi^*)$ unoccupied molecular orbital. The S(LVV) Auger cross section $\sigma_A(h\nu)$ has a maximum near 176 eV and slowly decreases at higher energies, following the electron-loss curve quite well.

The $\beta_A(h\nu)$ results for the S(LVV) channel are also presented in Fig. 22. The $\beta_A(h\nu)$ parameter includes contributions from some OCS

valence channels which could not be resolved. The asymmetry parameter is slightly positive below the S 2p threshold in the region of the discrete resonances. Above threshold, scatter in the data precludes any strong conclusions, although some structure might be present. In general, we observe a slow decrease in $\beta_A(h\nu)$ from 165 to 190 eV, which is consistent with valence contributions becoming less important as the Auger yield increases in this energy range.

The S 2p photoelectron results are shown in Fig. 23. In the top panel the results of Wight and Brion[11] are shown. The cross section of the S 2p photoelectron channel has a maximum at 176 eV and slowly decreases over the rest of the energy range. The discussion of the S(LVV) cross section for photon energies above the sulfur $L_{2,3}$ edges is also applicable to the S 2p channel.

The OCS S 2p asymmetry parameter is presented in the bottom panel of Fig. 23. The changes of the S 2p asymmetry parameter near 179 and 185 eV suggest that $\beta(\epsilon)$ might be affected near the thresholds of shake-up states, possibly as a result of autoionization. Allan et al.[37] have shown that S 2p shake-up states lie 9.6 and 15.3 eV above the sulfur $L_{2,3}$ edges in OCS. Wight and Brion[11] reported a feature near 191 eV which they suggested might be caused by shake-up structure. We have determined that the binding energies of these states are about 9.5(3) eV and 15.0(3) eV above the sulfur 2p edges with intensities that are 6.3(6)% and 11.7(7)% of the S 2p peak, respectively. Using Mg Kα radiation, Allan et al.[37] found that the shake-up peaks were 4.8(1.5)% and 6.4(2.4)% of the intensity of the S 2p peak, respectively.

VII. Conclusions

Many conclusions could be drawn from our experimental studies of the carbon K-shells of CO, CO_2, CF_4, and OCS, the oxygen K-shells of CO and CO_2, and the S 2p shell of OCS. The following conclusions are representative rather than exhaustive.

Shape resonances were observed in both the cross section and asymmetry parameter for the C 1s photoionization channels in each molecule. The C 1s cross section and asymmetry parameter for CO_2 show the most dramatic effects in the ℓ=2,3 continuum channels. The C 1s measurements of OCS may show two shape resonances, where ℓ=3,4 partial waves would be the successive dominant ionic channels. The C 1s results of CF_4 also are interpreted as shape-resonance phenomena, although no theoretical predictions are available.

The C(KVV) partial cross sections show both discrete resonances below the C 1s ionization thresholds and shape resonances in the continuum. The Auger asymmetry parameter shows no strong alignment at the π discrete resonances of CO, CO_2, and OCS and the $3sa_1$ resonance of CF_4. Two alternative explanations were offered; the spectator-electron model is the more appealing. Higher-resolution experiments are clearly needed. The CO C(KVV) Auger peak shows a small net alignment between the largest discrete resonance and the C 1s ionization threshold which may be caused by other discrete resonances. The shape resonances have little or no effect in the continuum region on $\beta_A(h\nu)$ in all the molecules. Small, but

nonzero, asymmetries are observed, but residual valence-shell interference cannot be ruled out.

The partial cross sections for the O(KVV) and O 1s peaks of CO and CO_2 show the O 1s shape resonance. The asymmetry parameter of the O(KVV) of CO may show an alignment near threshold.

The C 1s photoionization cross section of CO_2 given by the electron-ion coincidence measurements of Kay et al.[13] is in good agreement with our results, as are the electron-energy loss results of Wight et al.[7] and Wight and Brion[9-11] for the cross sections in the vicinity of the carbon K edge, oxygen K edge, and sulfur $L_{2,3}$ edges. The photoabsorption measurements of Barrus et al.[4] for the O 1s shell of CO and CO_2 are in excellent agreement with the present results.

The STMT partial cross sections of Padial et al.[16] for the C 1s and O 1s channels of CO are in excellent agreement with the present results. For CO_2, the C 1s shape resonance is located too close to threshold in theory,[17] and the O 1s cross section is only in qualitative agreement with the present results.

The partial cross sections and asymmetry parameters $\beta(\epsilon)$ predicted from the MSMXα calculations[32-34] are in qualitative agreement with the experimental results. This model works well in identifying possible shape-resonance features and in some cases predicts the location of the shape resonances in good agreement with the experimental measurements. Some discrepancies are noticed in particular for the O 1s asymmetries in CO and CO_2. The MSMXα

results of Grimm[34] using the localized-hole potential model is generally in better agreement with the results than is the unlocalized-hole potential model.

The HF static-exchange calculations by Lucchese and McKoy[18] for CO_2 show promise in correctly describing the C 1s asymmetry parameter. The C 1s photoionization cross section is predicted with the correct shape, but the maximum is located too close to threshold.

Acknowledgements

This work was supported by the Director, Office of Energy Research, Office of Basic Energy Sciences, Chemical Sciences of the U.S. Department of Energy under Contract No. DE-AC03-76SF00098. It was performed at the Stanford Synchrotron Radiation Laboratory, which was supported by the NSF through the Division of Materials Research.

References

1. C.N. Yang, Phys. Rev. 74, 764 (1948).
2. D. Dill, J.R. Swanson, S. Wallace, and J.L. Dehmer, Phys. Rev. Lett. 45, 1393 (1980).
3. C.M. Truesdale, S. Southworth, P.H. Kobrin, U. Becker, D.W. Lindle, H.G. Kerkhoff, and D.A. Shirley, Phys. Rev. Lett. 50, 1265 (1983).
4. D.M. Barrus, R.L. Blake, A.J. Burek, K.C. Chambers, and A.L. Pregenzer, Phys. Rev. A 20, 1045 (1979).
5. R.Z. Bachrach, F.C. Brown, A. Bianconi, and H. Petersen, Stanford Synchrotron Radiation Laboratory Report No. 77/16.
6. M. Tronc, G.C. King, R.C. Bradford, and F.H. Reed, J. Phys. B 9, L555 (1976).
7. G.R. Wight, C.E. Brion, and M.J. van der Wiel, J. Electron Spectrosc. Relat. Phenom. 1, 457 (1973).
8. M.J. van der Wiel, Th.M. El-Sherbini, and C.E. Brion, Chem. Phys. Lett. 7, 161 (1970).
9. G.R. Wight and C.E. Brion, J. Electron Spectrosc. Relat. Phenom. 3, 191 (1974).
10. G.R. Wight and C.E. Brion, J. Electron Spectrosc. Relat. Phenom. 4, 327 (1974).
11. G.R. Wight and C.E. Brion, J. Electron Spectrosc. Relat. Phenom. 4, 335 (1974).
12. A.P. Hitchcock and C.E. Brion, J. Electron Spectrosc. Relat. Phenom. 18, 1 (1980).

13. R.B. Kay, Ph.E. van der Leeuw, and M.J. van der Wiel, J. Phys. B 10, 2513 (1977).

14. J. Stohr, K. Baberschke, R. Jaeger, R. Treichler, and S. Brennan, Phys. Rev. Lett. 47, 381 (1981).

15. C.L. Allyn, T. Gustaffson, and E.W. Plummer, Chem. Phys. Lett. 4, 127 (1977); Solid State Commun. 24, 531 (1977).

16. N. Padial, G. Csanak, B.V. McKoy, and P.W. Langhoff, J. Chem. Phys. 69, 2982 (1978).

17. N. Padial, G. Csanak, B.V. McKoy, and P.W. Langhoff, Phys. Rev. A 23, 218 (1981).

18. R.R. Lucchese and B.V. McKoy, Phys. Rev. A 26, 1406 (1982).

19. M.G. White, R.A. Rosenberg, G. Gabor, E.D. Poliakoff, G. Thornton, S. Southworth, and D.A. Shirley, Rev. Sci. Instrum. 50, 1288 (1979).

20. F.C. Brown, R.Z. Bachrach, and N. Lien, Nucl. Instrum. Methods 152, 73 (1978).

21. S. Southworth, C.M. Truesdale, P.H. Kobrin, D.W. Lindle, W.D. Brewer, and D.A. Shirley, J. Chem. Phys. 76, 143 (1982).

22. F. Wuilleumier and M.O. Krause, J. Electron Spectrosc. Relat. Phenom. 15, 15 (1979).

23. K. Siegbahn, C. Nordling, G. Johannson, J. Hedman, P.F. Heden, K. Hamrin, U. Gelius, T. Bergmark, L.O. Werme, R. Manne, and V. Baer, ESCA Applied to Free Molecules, North-Holland Publ. Co., Amsterdam (1969).

24. W.E. Moddeman, T.A. Carlson, M.O. Krause, B.P. Pullen, W.E. Bull, and G.K. Schweitzer, J. Chem. Phys. 55, 2317 (1971).

25. J.A. Kelber, D.R. Jennison, and R.R. Rye, J. Chem. Phys. 75, 652 (1981).

26. H. Ågren, J. Chem. Phys. 75, 1267 (1981).

27. P.H. Kobrin, S. Southworth, C.M. Truesdale, D.W. Lindle, U. Becker and D.A. Shirley, Phys. Rev. A (in press).

28. T.D. Thomas, (private communication).

29. L. Ungier, J.K. Gimzewski, and T.D. Thomas, Proc. X-82 Conf. on X-ray and Atomic Inner-Shell Phys. Eugene, Abstracts, 245 (1982).

30. J.L. Dehmer and D. Dill, Phys. Rev. Lett., 35, 213 (1975).

31. J.L. Dehmer and D. Dill, J. Chem. Phys. 65, 5327 (1976).

32. D. Dill, S. Wallace, J. Siegel, and J.L. Dehmer, Phys. Rev. Lett. 42, 411 (1979).

33. J.L. Dehmer and D. Dill, Argonne National Laboratory Report (ANL-77-65) p. 65.

34. F.A. Grimm, Chem. Phys. 53, 71 (1980).

35. T.A. Carlson, M.O. Krause, and W.E. Moddeman, J. de Physique 32, C4-76 (1971).

36. L.J. Aarons, M. Barber, M.F. Guest, I.H. Hillier, and J.H. Mc Cartney, Mol. Phys. 26, 1247 (1973).

37. C.J. Allan, U. Gelius, D.A. Allison, G. Johansson, H. Siegbahn, and K. Siegbahn, J. Electron Spectrosc. Relat. Phenom. 1, 131 (1973).

38. C.R. Brundle, M.B. Robin, and H. Basch, J. Chem. Phys. 53, 2196 (1970).

39. L.N. Mazlov, A. P. Sadovskii, V.M. Bertenev, K.E. Mironov, T.I. Guzhavina, and L.I. Chernyavskii, Zh. Struct. Chem. 13, 859 (1972); (J. Struct. Chem. 13, 802 (1972)).

40. A.S. Vinogradov and T.M. Zimkina, Opt. Spectrosk. 31, 685 (1971) (Opt. Spectrosc. (U.S.S.R.) 31, 364 (1971)).

Table I. Total O 1s shake-up intensity relative to the O 1s main line of CO_2. Numbers in parentheses represent errors in the last digit.

hν(eV)	branching ratio(%)
593.0	17(2)
609.0	20(3)
615.0	24(3)
625.0	21(2)
631.0	22(3)

Figure Captions

Figure 1. TOF spectrum from CO, after conversion to a kinetic-energy scale. The sample was irradiated with 305.8 eV photons (first-order), with some 2nd- and 3rd-order radiation also present. Auger peaks are labelled B-1, etc., following the notation of Moddeman et al. (Ref. 24) (see text for details). For this spectrum the electrons were retarded by 150 volts over part of their flight path.

Figure 2. TOF spectrum similar to Fig. 1, but with $h\nu$ = 315.0 eV and a retarding voltage of 5 volts, allowing the C 1s and O 1s (2nd-order) peaks to be recorded.

Figure 3. C(KVV) Auger results for CO. Top panel: open circles show the total Auger intensity scaled to the results of Tronc et al., Ref. 6. The π resonance at $h\nu$ = 287.3 eV is evident. Filled circles show the region above $h\nu$ = 290 eV, expanded 16 times. The dashed curve represents the C 1s electron-ion coincidence measurements of Kay et al., Ref. 13, also x16. Bottom panel: filled circles show our asymmetry-parameter results. The solid curve shows the orientation parameter β_m calculated by Dill et al., Ref. 2.

Figure 4. CO C(KVV) Auger spectra taken at the π resonance ($h\nu$ = 287.3 eV) below the C 1s threshold with a retarding potential of 100 volts, and at $h\nu$ = 296.8 eV above the C 1s threshold with a 150 volt retarding potential. The low-energy shoulder on the 265-eV peak in the top spectrum is due to

C(KVV) Auger transitions other than B-1 (see Fig. 1). Assignments of unlabeled features in the bottom spectrum can be found in Fig. 1.

Figure 5. The C 1s photoelectron results for CO. Top panel: our $\sigma(\varepsilon)$ values are represented by filled circles, while open circles show the electron-ion coincidence results of Kay et al., Ref. 13. The solid curve shows the STMT calculation of Padial et al., Ref. 16, and the dashed curve the MSMXα calculation by Dehmer and Dill, Ref. 33. Bottom panel: filled circles show our asymmetry results. The solid and dashed curves are results from localized-hole MSMXα calculations by Dill et al., Ref. 32, and Grimm, Ref. 34, respectively.

Figure 6. The O(KVV) results for CO. Top panel: experimental cross section (points) and the absorption results of Barrus et al., Ref. 4 (solid curve). Bottom panel: asymmetry parameter (points) and the β_m curve given by Dill et al., Ref. 2.

Figure 7. The O 1s results for CO. Top panel: cross-section results. Filled circles are our data, open circles represent the absorption results of Barrus et al., Ref. 4, and the solid curve represents the STMT calculation of Padial et al., Ref. 16. Bottom panel: asymmetry parameter (points), compared with localized-hole MSMXα calculations by Grimm, Ref. 34 (solid curve), and by Dill et al., Ref. 32 (dashed curve).

Figure 8. TOF spectrum of CO expanded around the O 1s peak. Shake-up structure, labelled "S", has an intensity of 13(3)% relative to the main peak.

Figure 9. TOF spectrum of CO_2 at a photon energy of 331.6 eV, after conversion to a linear energy scale. The peaks are labeled as in Figs. 1 and 2. The shoulder on B-5 contains other C(KVV) Auger peaks, and the peak at ~300 eV is from valence photoelectrons.

Figure 10. The C(KVV) Auger results for CO_2. Top panel: present results for the cross section (filled circles) and electron-energy loss results of Wight and Brion, Ref. 9 (dotted curve), to which our data were normalized at 315 eV. Bottom panel: asymmetry parameter.

Figure 11. The C 1s results for CO_2. Top panel: cross section. Filled circles are present results, open circles the electron-energy loss results of Wight and Brion, Ref. 9, the dashed curve is the STMT prediction by Padial et al., Ref. 17, and the solid curve represents the HF static-exchange calculation by Lucchese and McKoy, Ref. 18. Bottom panel: asymmetry parameter. Filled circles are present results, the solid curve is the HF calculation of Lucchese and McKoy, the dotted and dashed curve are the localized-hole and unlocalized hole MSMXα calculations, respectively, by Grimm, Ref. 34.

Figure 12. Results for the O(KVV) peak in CO_2. Top panel: cross

section. Filled circles are present results, and open circles are photoabsorption results of Barrus et al., Ref. 4. The dashed and full curves display the theoretical calculations by Padial et al., Ref. 17, and by Lucchese and McKoy, Ref. 18, respectively. Bottom panel: asymmetry parameter.

Figure 13. Asymmetry parameter for the O 1s peak in CO_2. The present results are shown as points. The solid and dashed curves represent predictions from localized-hole MSMXα calculations by Grimm, Ref. 34, and Dill et al., Ref. 32, respectively.

Figure 14. The O 1s peaks of CO_2 on an expanded scale, to show shake-up structure.

Figure 15. TOF spectrum from CF_4 excited with a photon energy of 318.8 eV. The peaks are (left to right): C 1s, C(KVV) plus inner-valence states, $4a_1 + 3t_2$, $1e + 4t_2 + 1t_1$, C 1s (second-order), and F(KVV) (third-order).

Figure 16. The CF_4 C(KVV) results, shown as filled circles. Top panel: the cross-section curve of Bachrach et al., Ref. 5, corrected for valence-electron contributions to the photoabsorption cross section, is shown as a solid curve. Our data were normalized to this curve at 302 eV. Bottom panel: asymmetry parameter.

Figure 17. The C 1s photoelectron results for CF_4. Our data are shown as filled circles. Open circles in the top panel

show some of the electron-energy loss results of Wight and Brion, Ref. 10, to which our data are normalized at 310 eV. The solid curve represents photoabsorption results by Bachrach et al., Ref. 5.

Figure 18. TOF spectrum of OCS excited at a photon energy of 311.0 eV. The peaks are (left to right): C 1s, S 2s ($6\sigma^{-1}$), S 2p (with the left shoulder being the S(LVV) Auger peak), C(KVV) Auger plus valence states, and O(KVV) Auger.

Figure 19. TOF spectrum of OCS excited at a photon energy of 179.0 eV. Four photon pulses separated by 2.8 ns were present, which caused the S(LVV) Auger peak to appear as four structures and the S 2p peak to be broadened.

Figure 20. Cross section and asymmetry parameter for the C(KVV) Auger electrons of OCS. Some valence intensity is included in the results. The solid curves in the top panel represent the electron-energy loss results of Wight and Brion, Ref. 11, and the present measurements correspond to the filled circles. The measured asymmetry parameter is shown in the bottom panel.

Figure 21. Cross section and asymmetry parameter for the C 1s shell of OCS. The relative cross section is shown in the top panel. The measured asymmetry parameter, shown by the filled circles, and the localized-hole MSMXα calculation of Grimm, Ref. 34 (lowered by 0.3β units for comparison) (solid curve), are shown in the bottom panel.

Figure 22. The S(LVV) results from OCS. Our data are represented by filled circles in both panels. Open circles in the top panel are electron-energy loss results of Wight and Brion, Ref. 11, scaled to our data. Solid curves are drawn to guide the eye.

Figure 23. The S 2p results from OCS. The notation is the same as in Fig. 22. Note that $\beta(\epsilon)$ is plotted on an expanded scale.

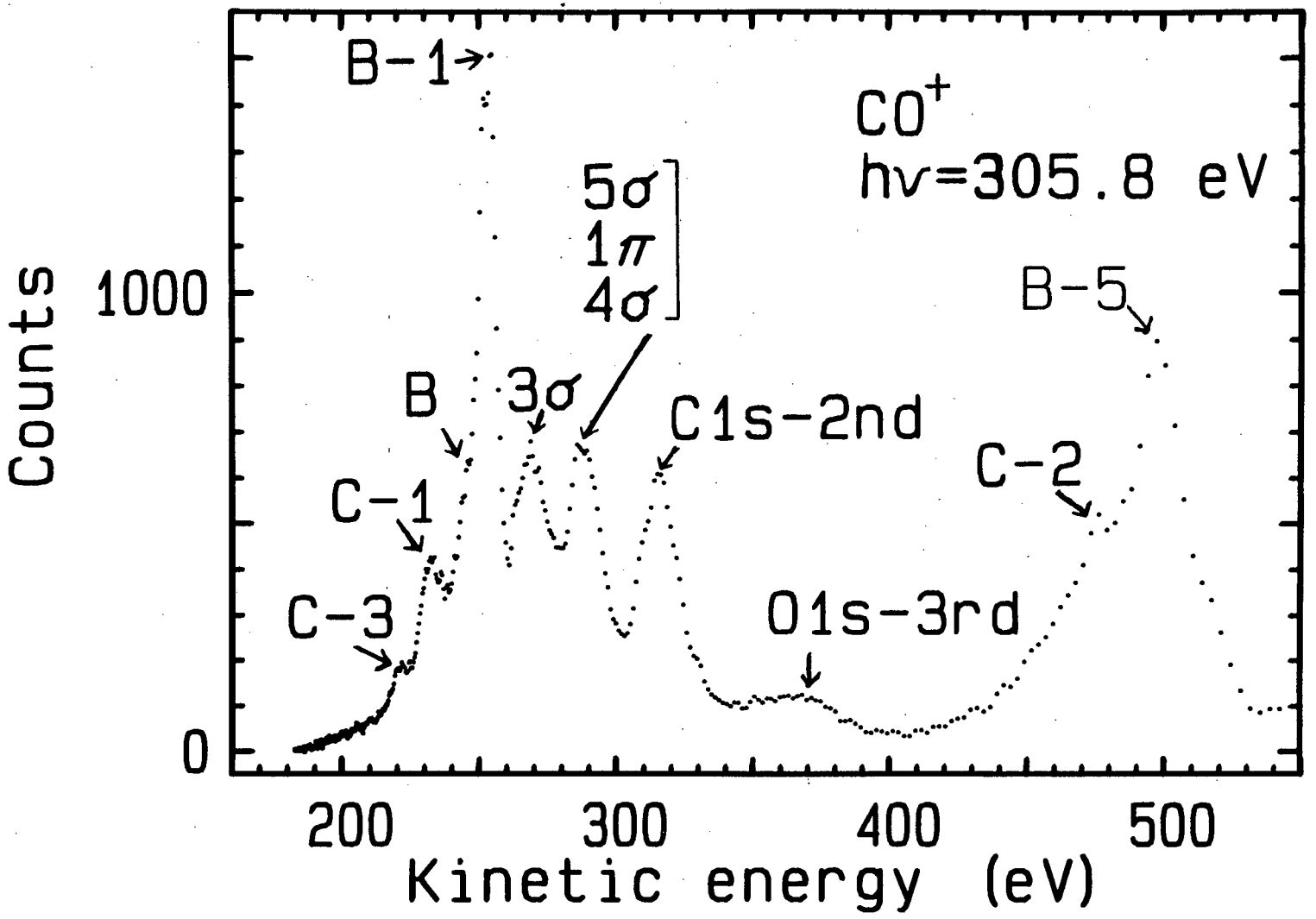

XBL 831-7879

Figure 1

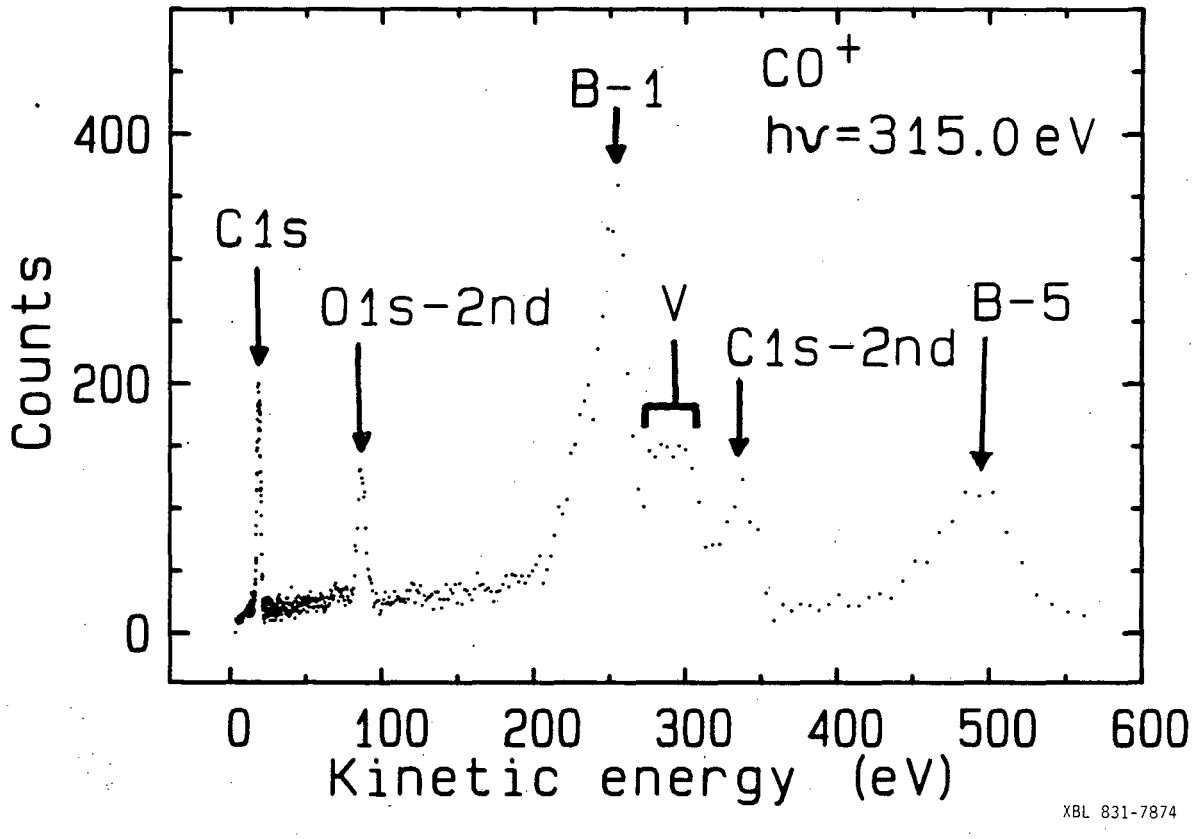
CO+
hν=315.0 eV
B-1
C1s
O1s-2nd
V
C1s-2nd
B-5
Counts
400
200
0
0
100
200
300
400
500
600
Kinetic energy (eV)
XBL 831-7874

Figure 2

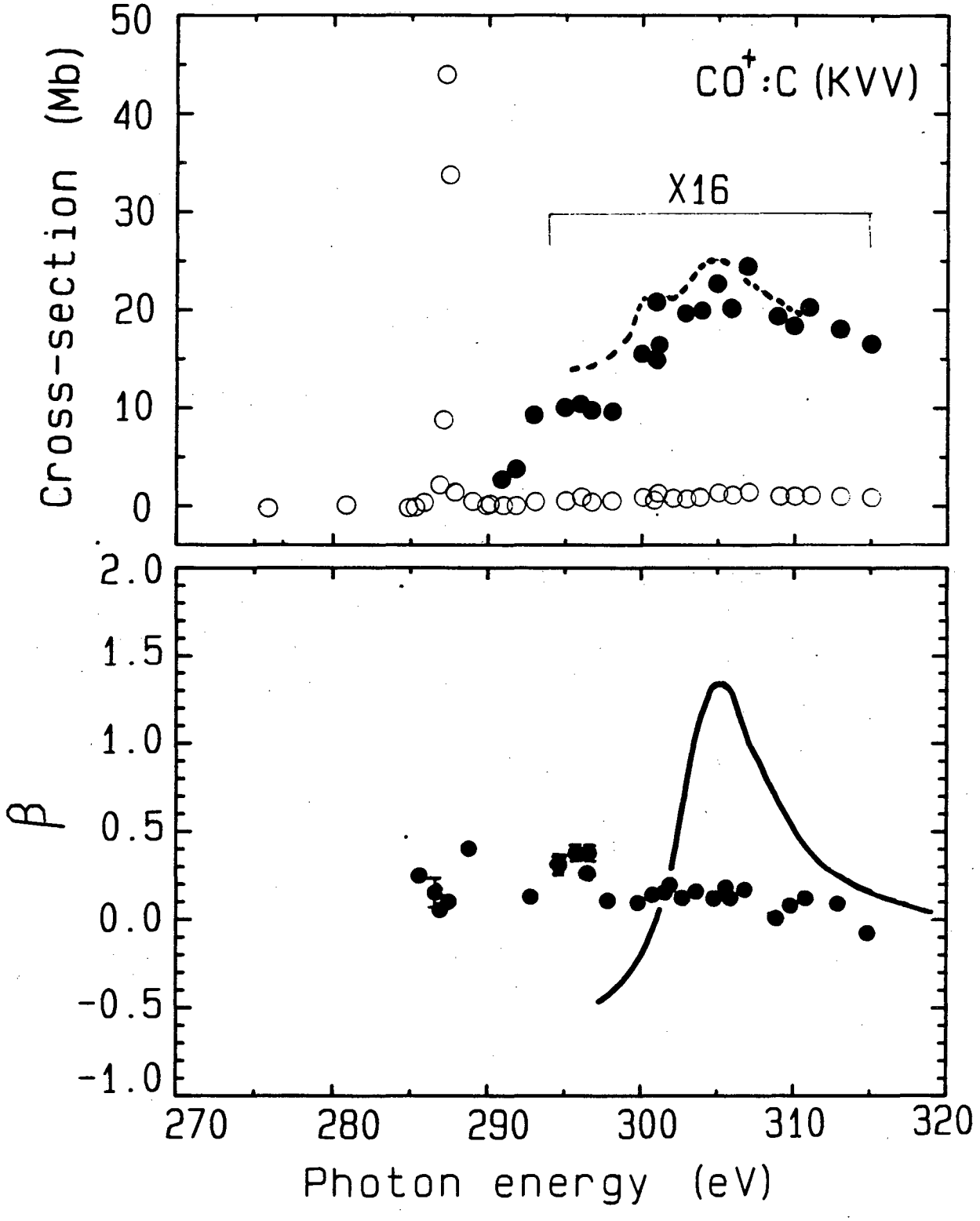
Cross-section (Mb)
50
40
30
20
10
0
CO^+:C (KVV)
X16
2.0
1.5
1.0
0.5
0.0
-0.5
-1.0
β
270
280
290
300
310
320
Photon energy (eV)
XBL 8212-12256

Figure 3

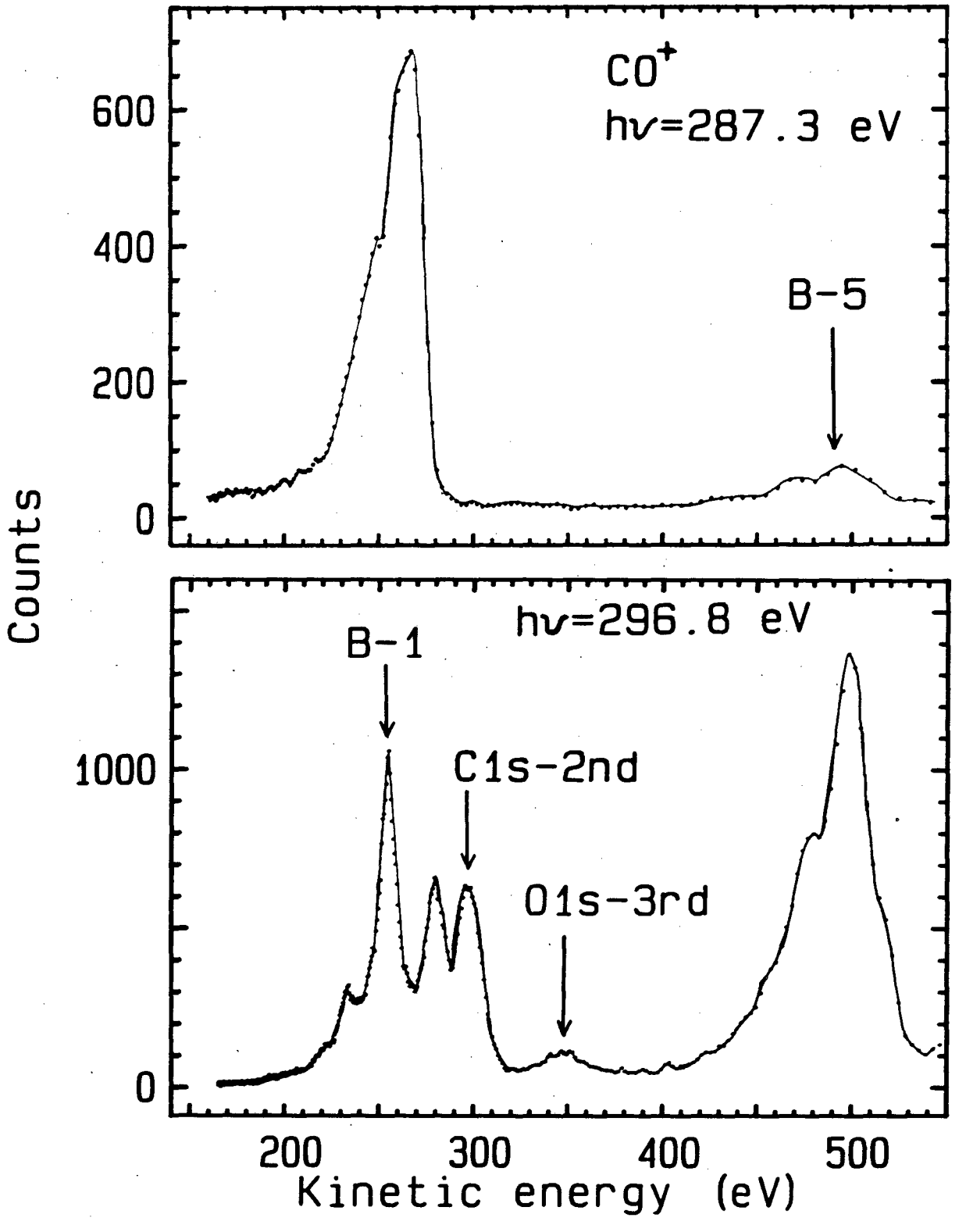
CO+
hν=287.3 eV
B-5
600
400
200
0
hν=296.8 eV
B-1
C1s-2nd
O1s-3rd
1000
0
Counts
200
300
400
500
Kinetic energy (eV)
XBL 832-8338

Figure 4

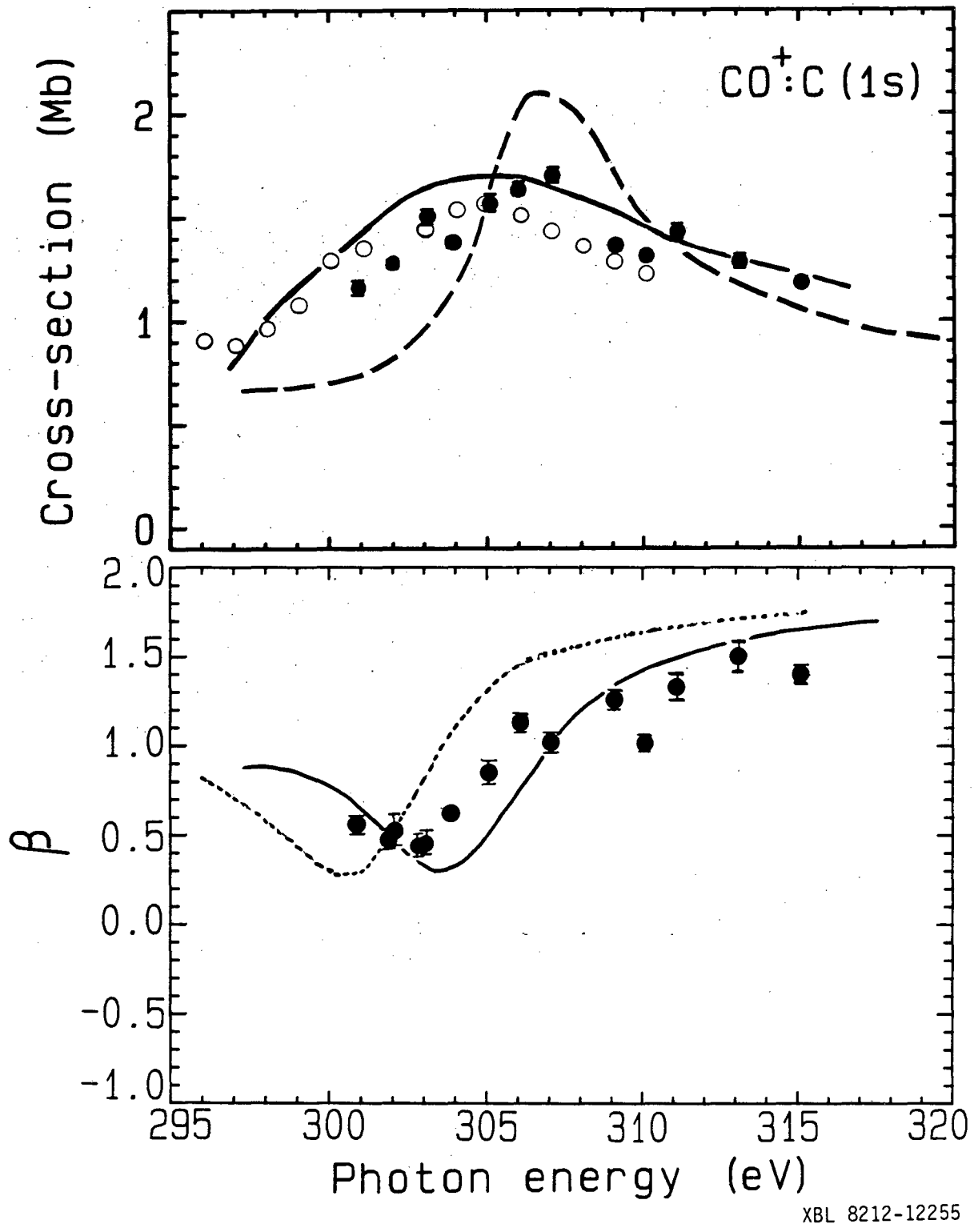
CO^+:C (1s)
Cross-section (Mb)
0
1
2
β
2.0
1.5
1.0
0.5
0.0
-0.5
-1.0
295
300
305
310
315
320
Photon energy (eV)
XBL 8212-12255

Figure 5

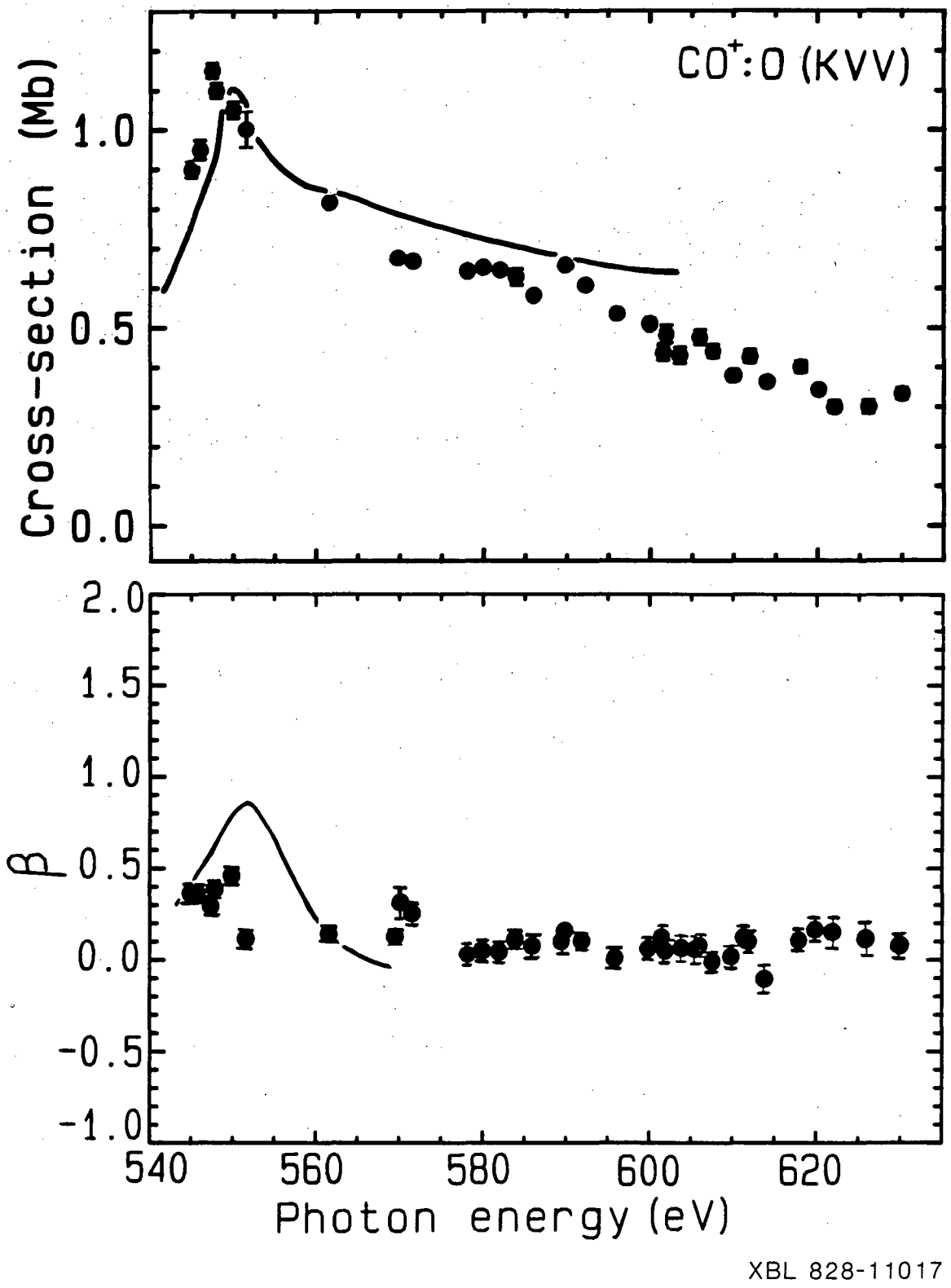
CO+:O (KVV)
Cross-section (Mb)
1.0
0.5
0.0
2.0
1.5
1.0
0.5
0.0
-0.5
-1.0
β
540
560
580
600
620
Photon energy (eV)
XBL 828-11017

Figure 6

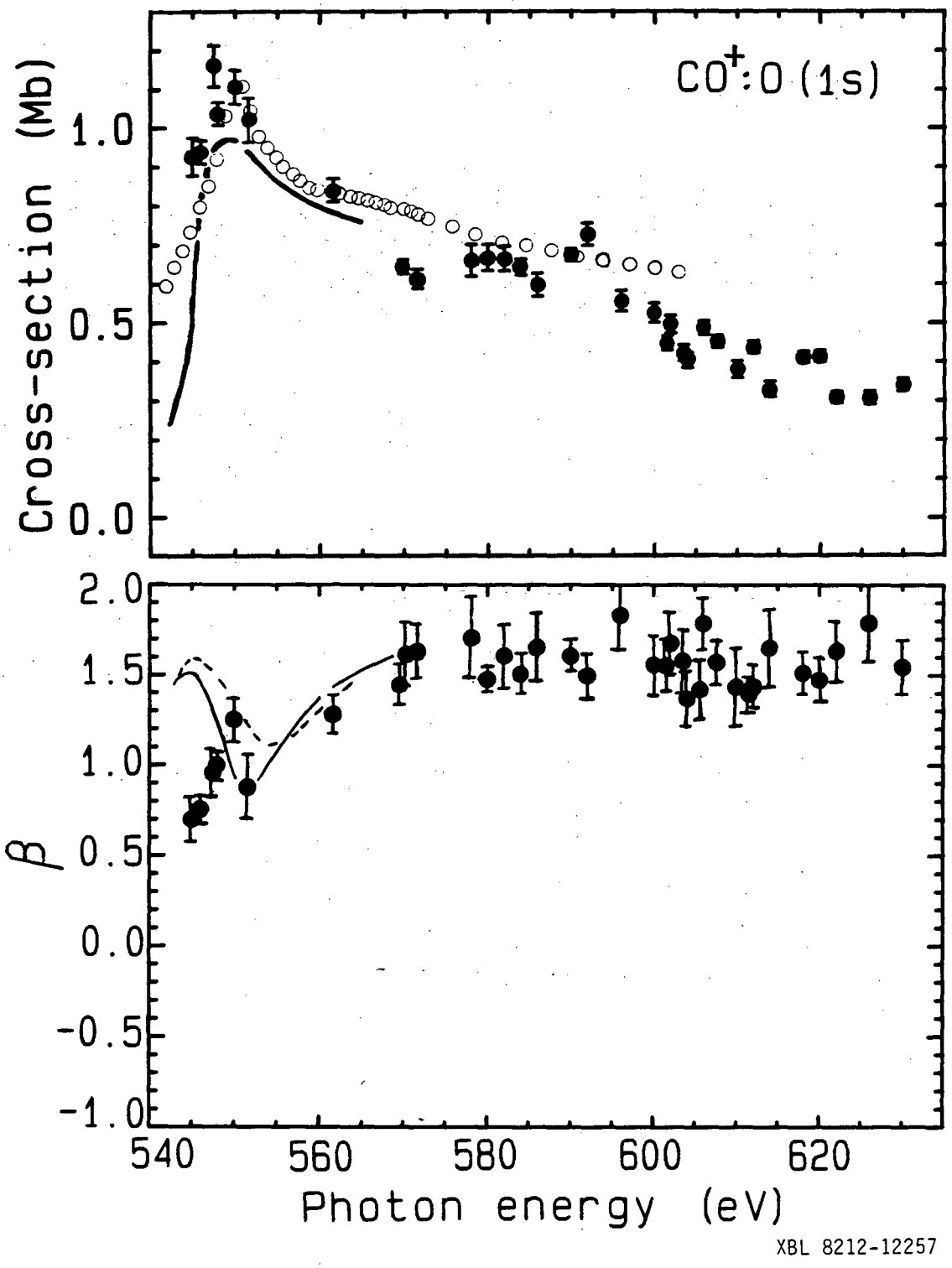
CO+:O (1s)
Cross-section (Mb)
1.0
0.5
0.0
2.0
1.5
1.0
0.5
0.0
-0.5
-1.0
β
540
560
580
600
620
Photon energy (eV)
XBL 8212-12257

Figure 7

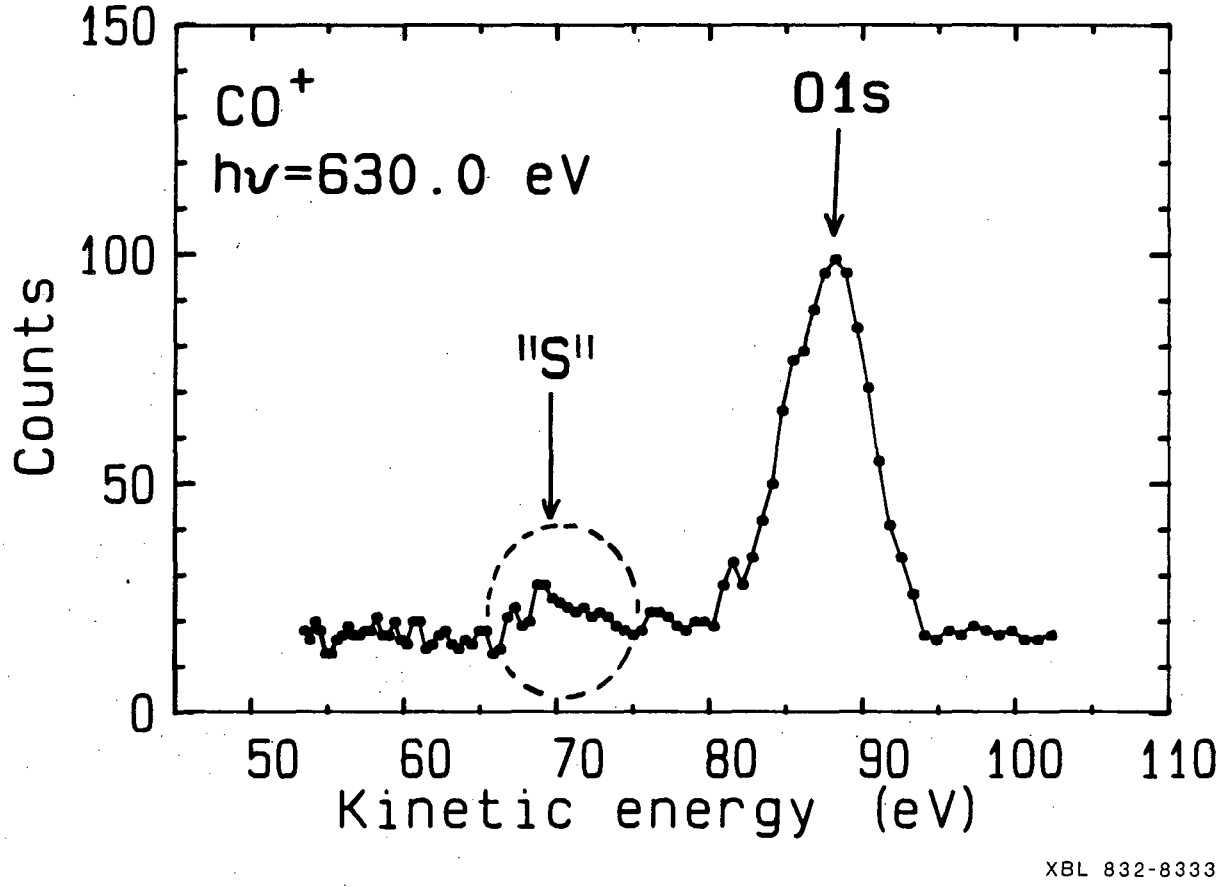
150
100
50
0
Counts
CO^+
hν=630.0 eV
O1s
"S"
50
60
70
80
90
100
110
Kinetic energy (eV)
XBL 832-8333

Figure 8

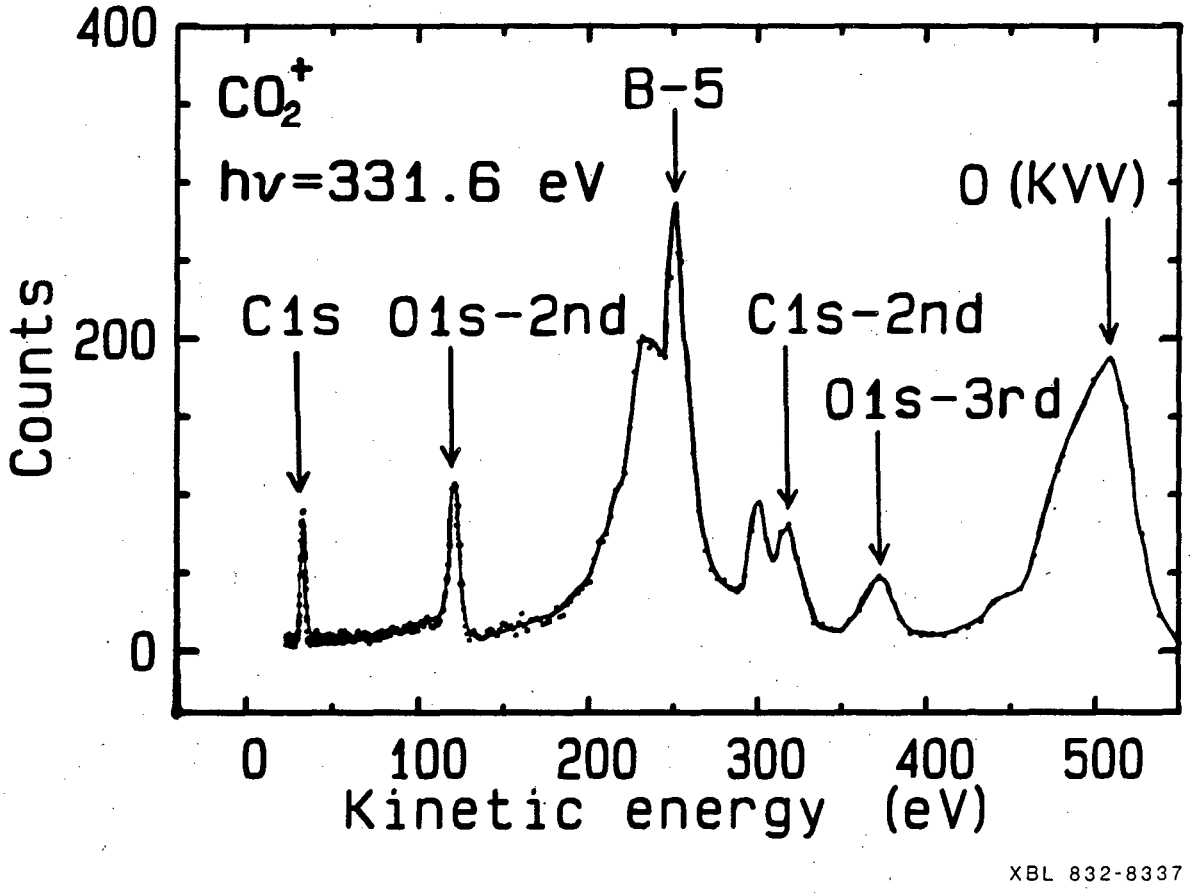
400
200
0
Counts
CO_2^+
hν=331.6 eV
B-5
O (KVV)
C1s
O1s-2nd
C1s-2nd
O1s-3rd
0
100
200
300
400
500
Kinetic energy (eV)
XBL 832-8337

Figure 9

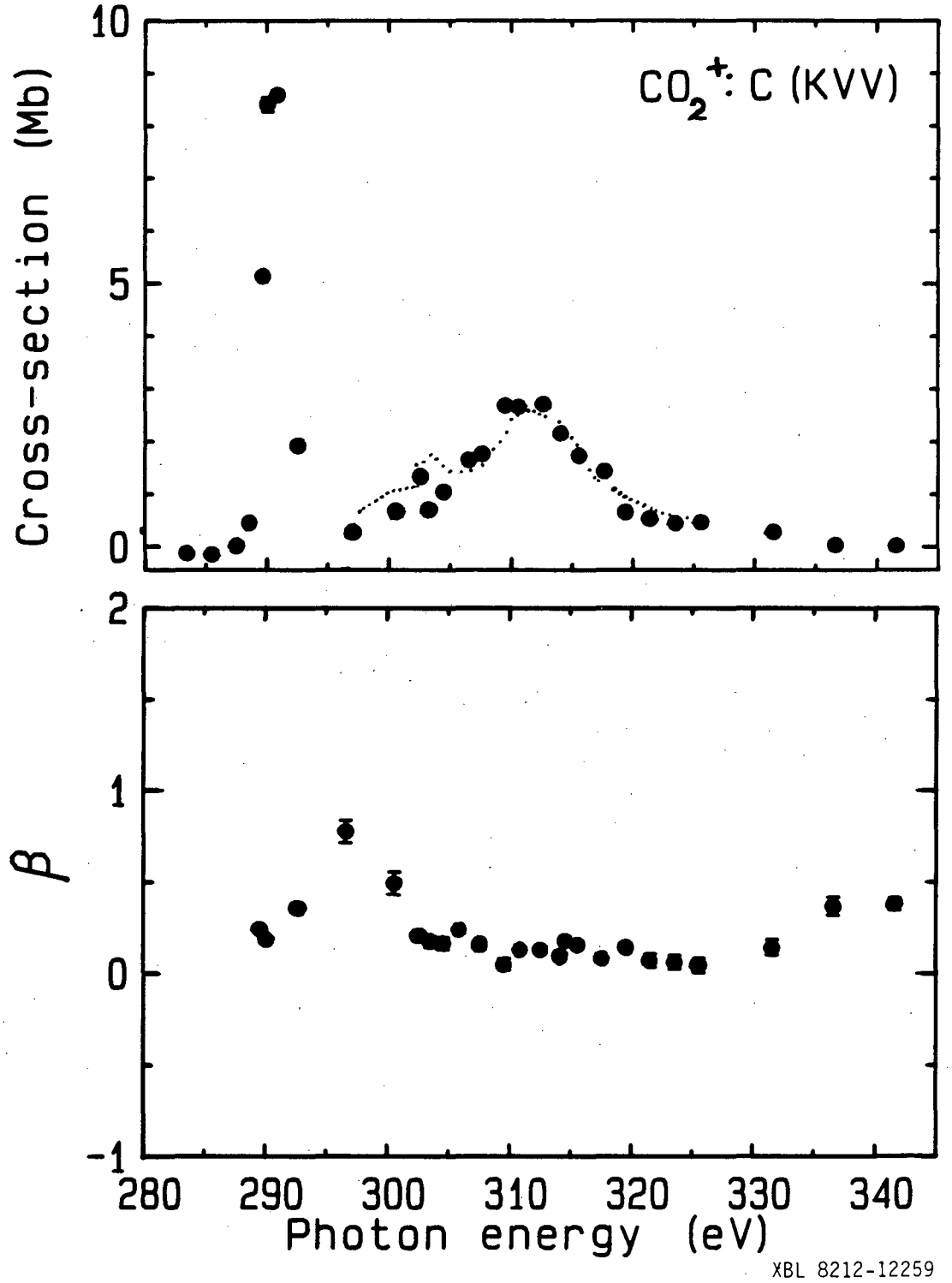
CO_2^+: C (KVV)
Cross-section (Mb)
10
5
0
β
2
1
0
-1
280
290
300
310
320
330
340
Photon energy (eV)
XBL 8212-12259

Figure 10

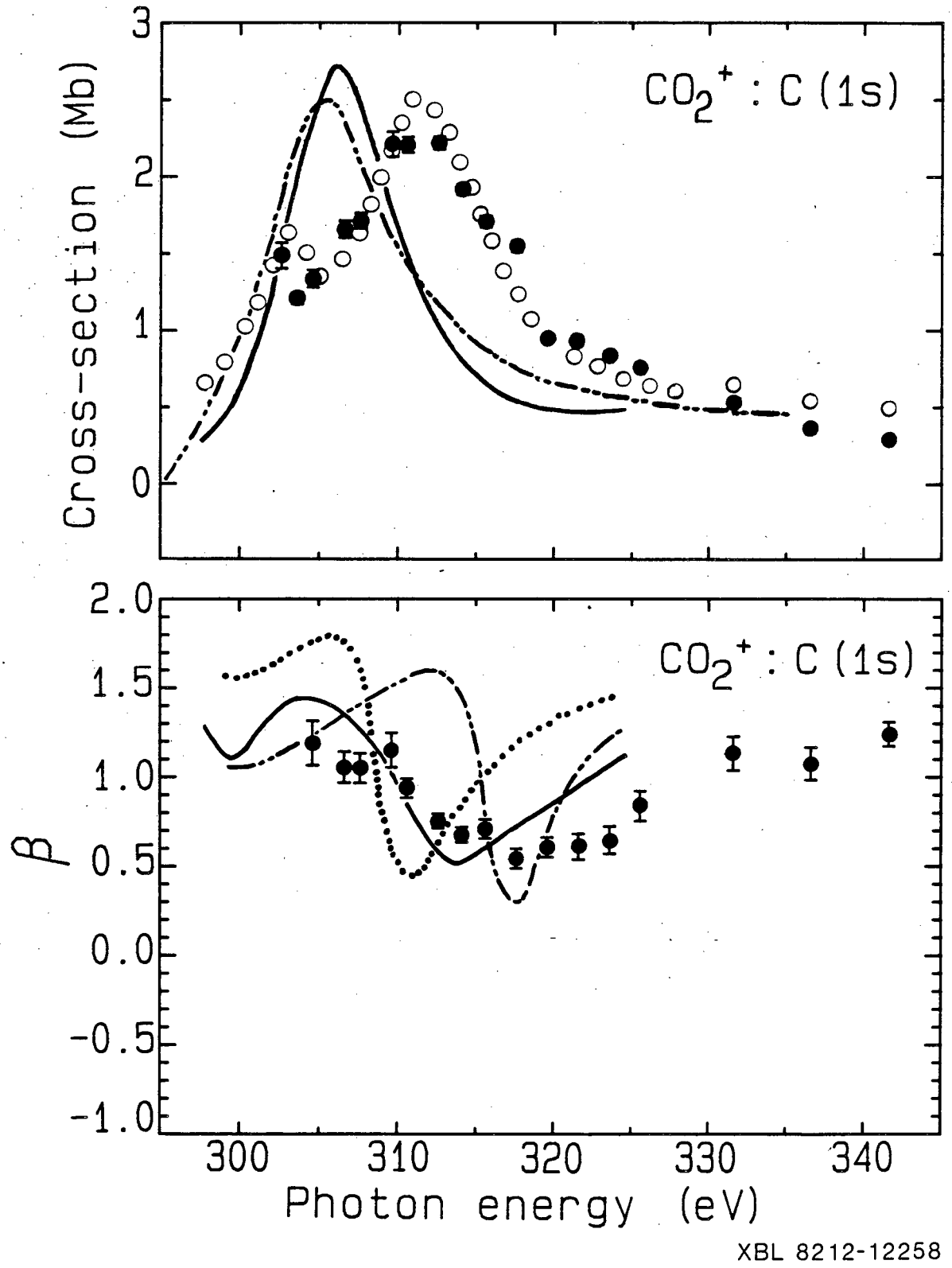
Cross-section (Mb)
CO_2^+ : C (1s)
β
CO_2^+ : C (1s)
Photon energy (eV)
XBL 8212-12258

Figure 11

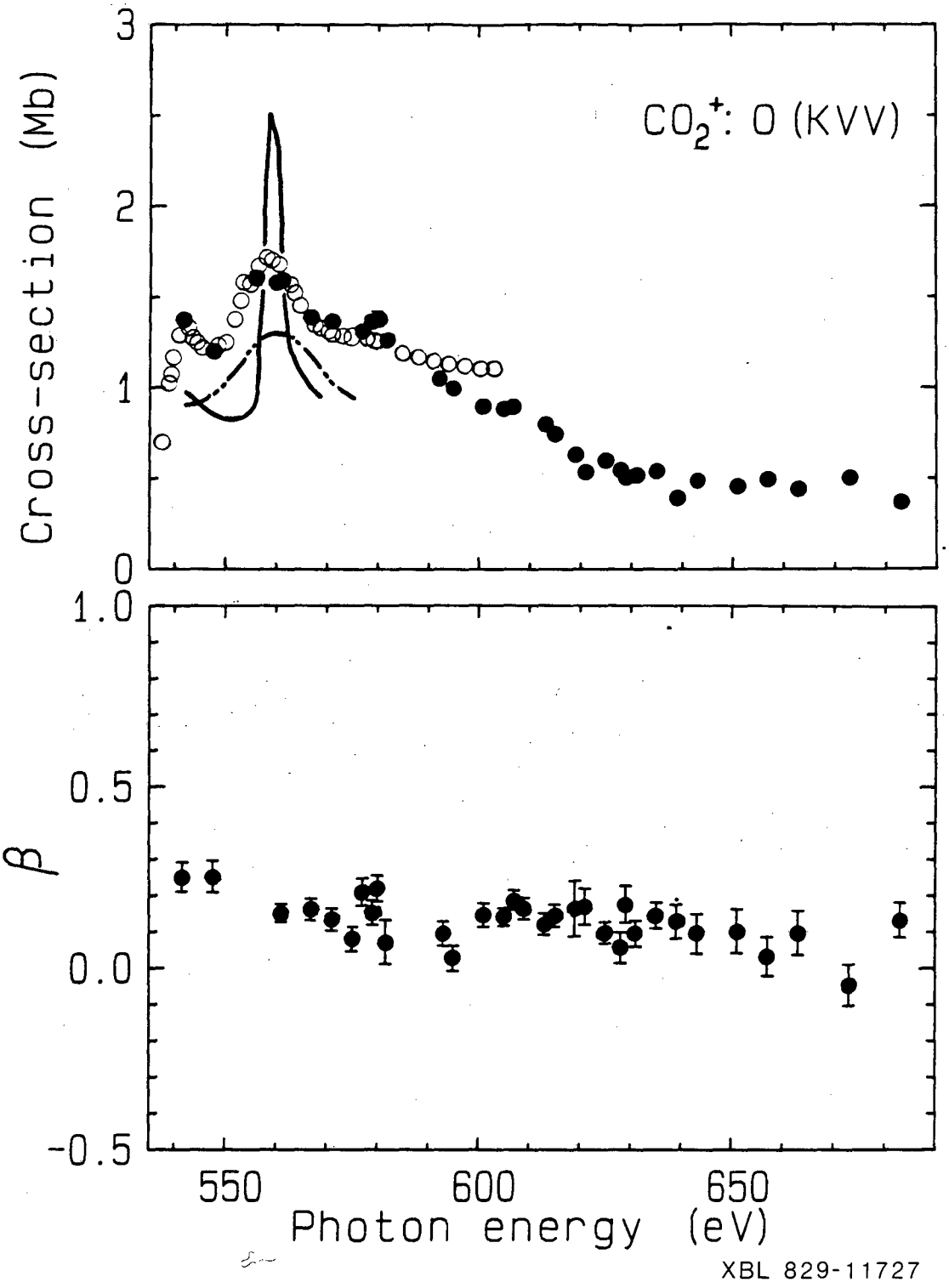
CO_2^+: O (KVV)
Cross-section (Mb)
3
2
1
0
1.0
0.5
0.0
-0.5
β
550
600
650
Photon energy (eV)
XBL 829-11727

Figure 12

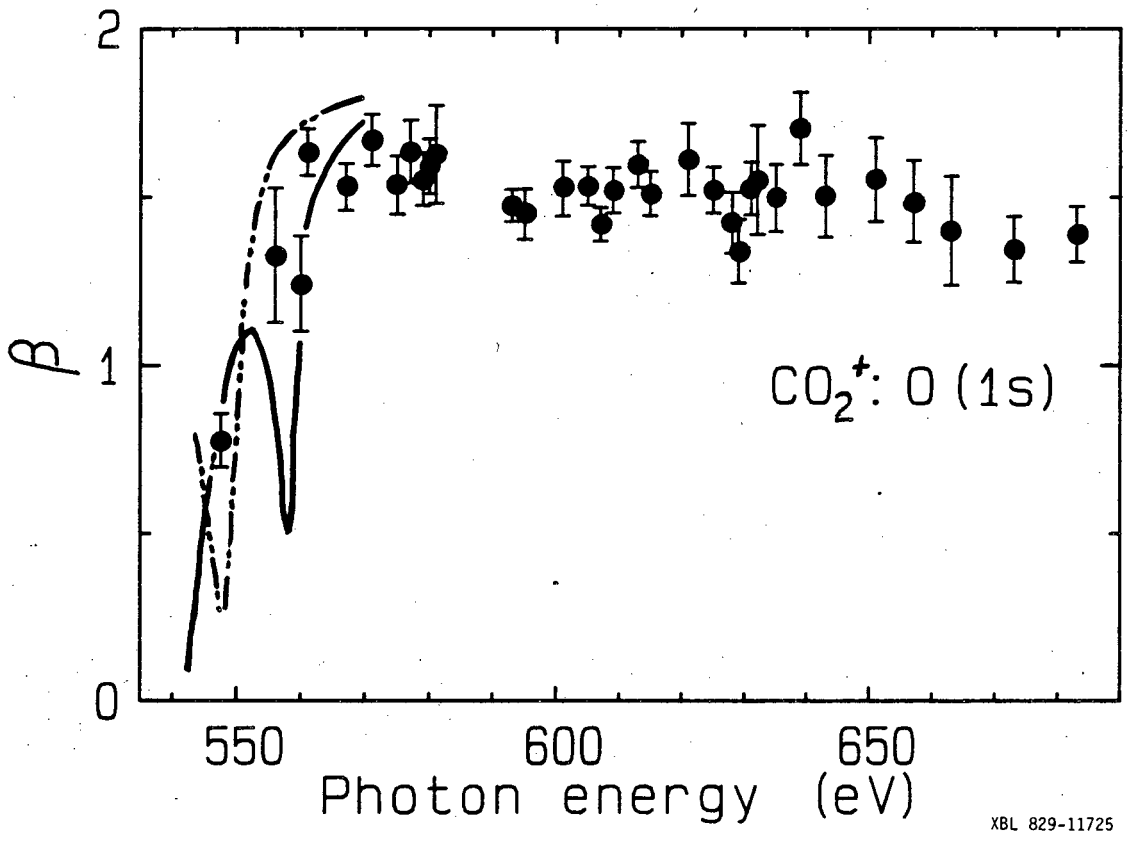

Figure 13

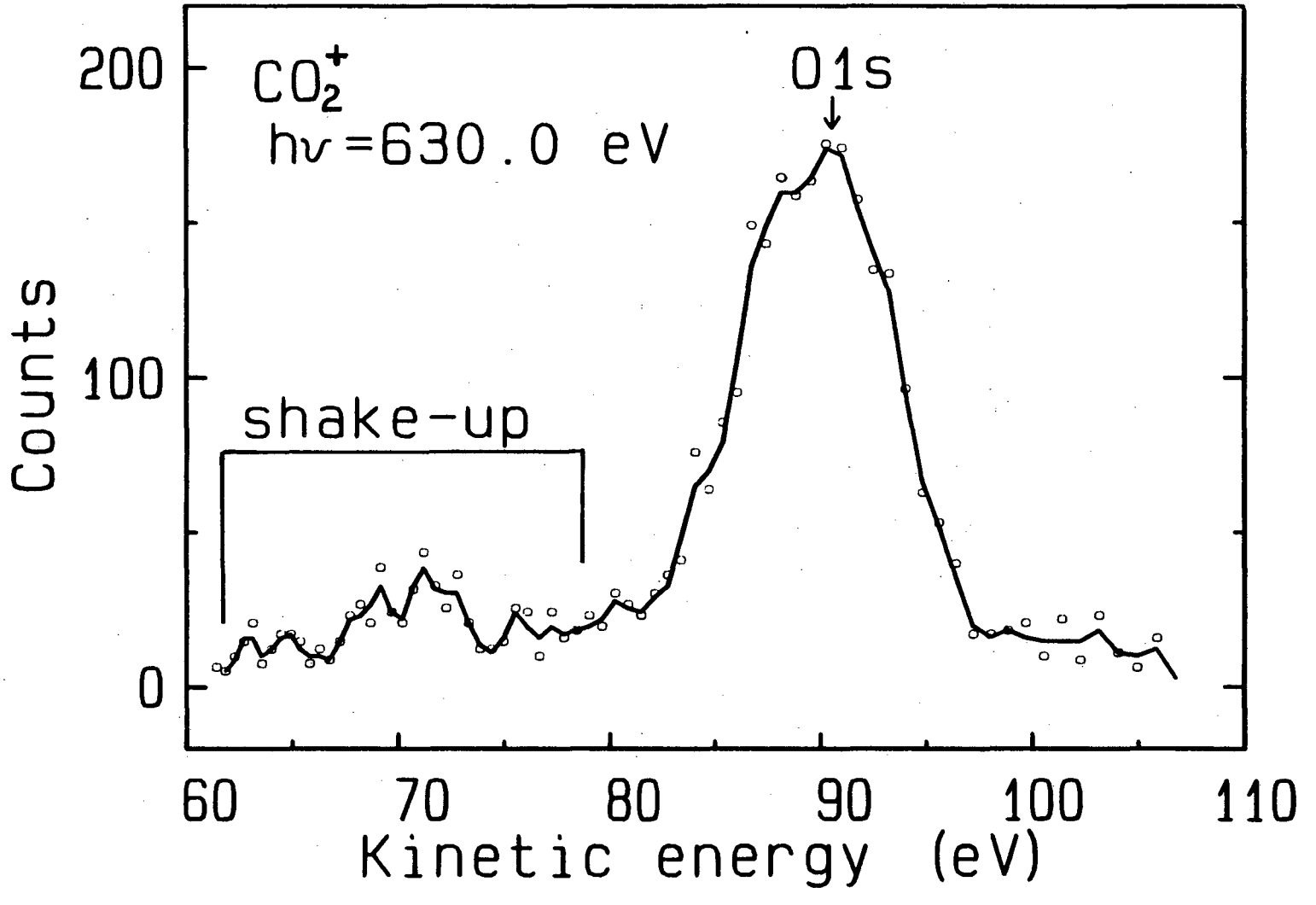

XBL 831-7881

Figure 14

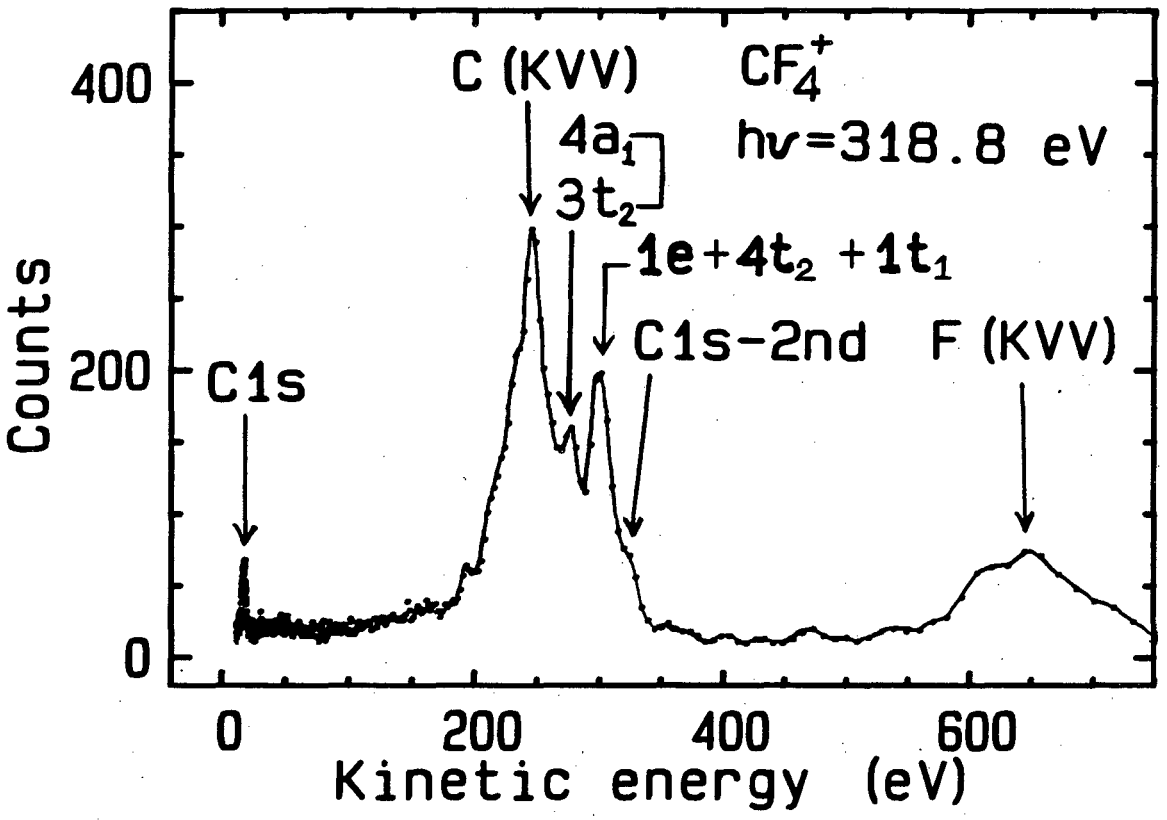
400
200
0
Counts
C (KVV)
CF_4^+
$4a_1$
$3t_2$
hν=318.8 eV
$1e+4t_2+1t_1$
C1s-2nd
F (KVV)
C1s
0
200
400
600
Kinetic energy (eV)
XBL 832-8334

Figure 15

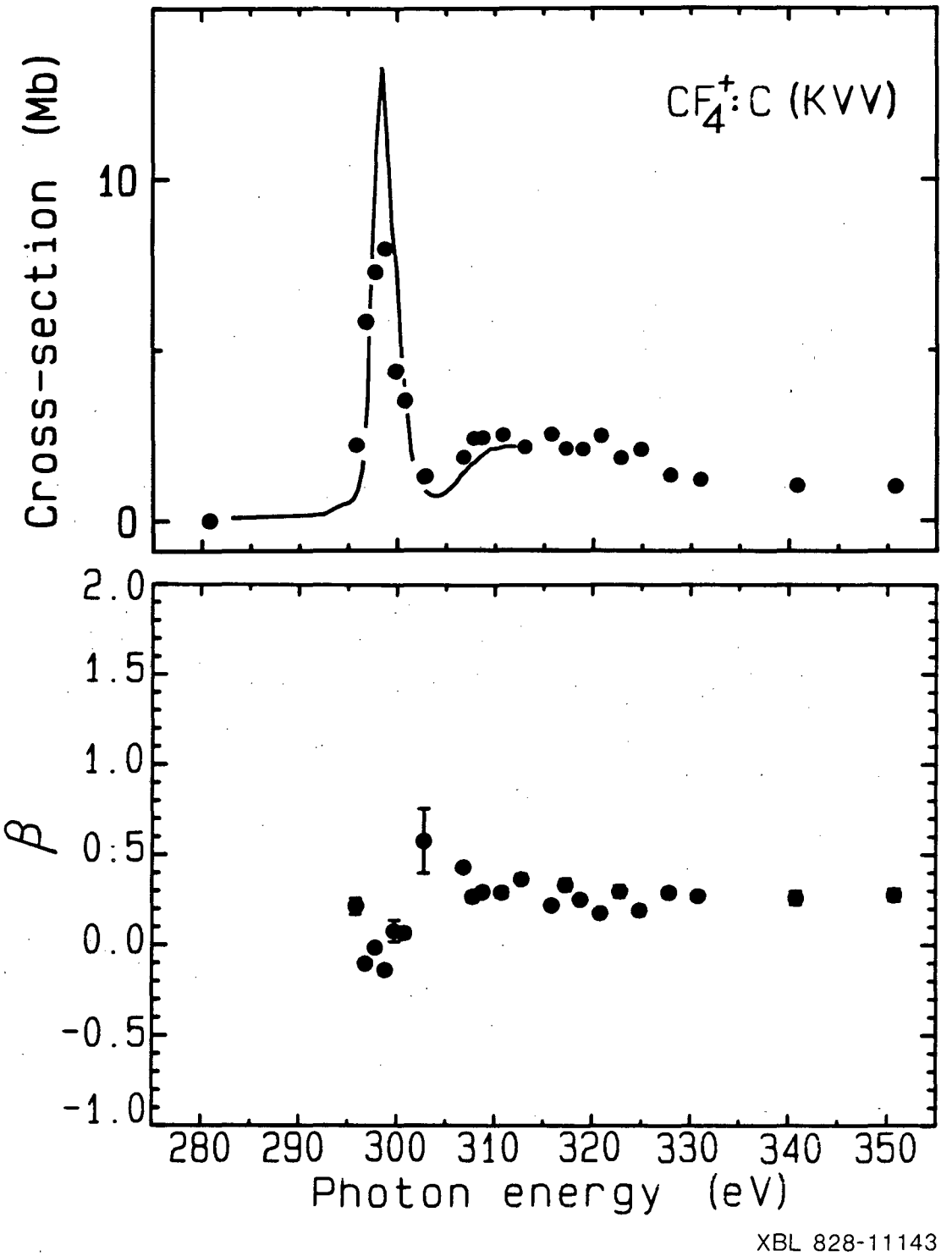
CF_4^+: C (KVV)
Cross-section (Mb)
10
0
2.0
1.5
1.0
0.5
0.0
-0.5
-1.0
β
280 290 300 310 320 330 340 350
Photon energy (eV)
XBL 828-11143

Figure 16

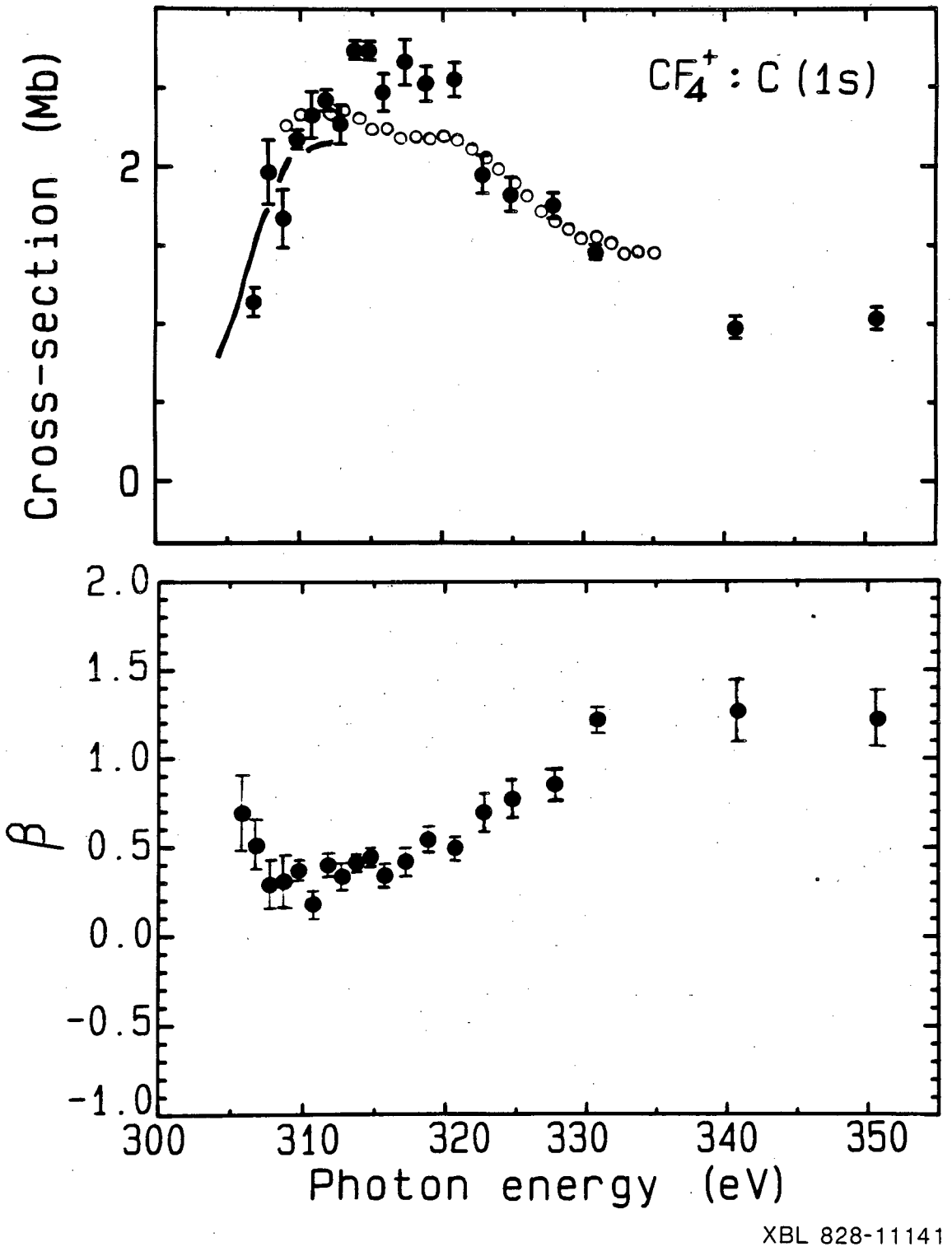
Cross-section (Mb)
CF_4^+ : C (1s)
2
0
2.0
1.5
1.0
0.5
0.0
-0.5
-1.0
β
300
310
320
330
340
350
Photon energy (eV)
XBL 828-11141

Figure 17

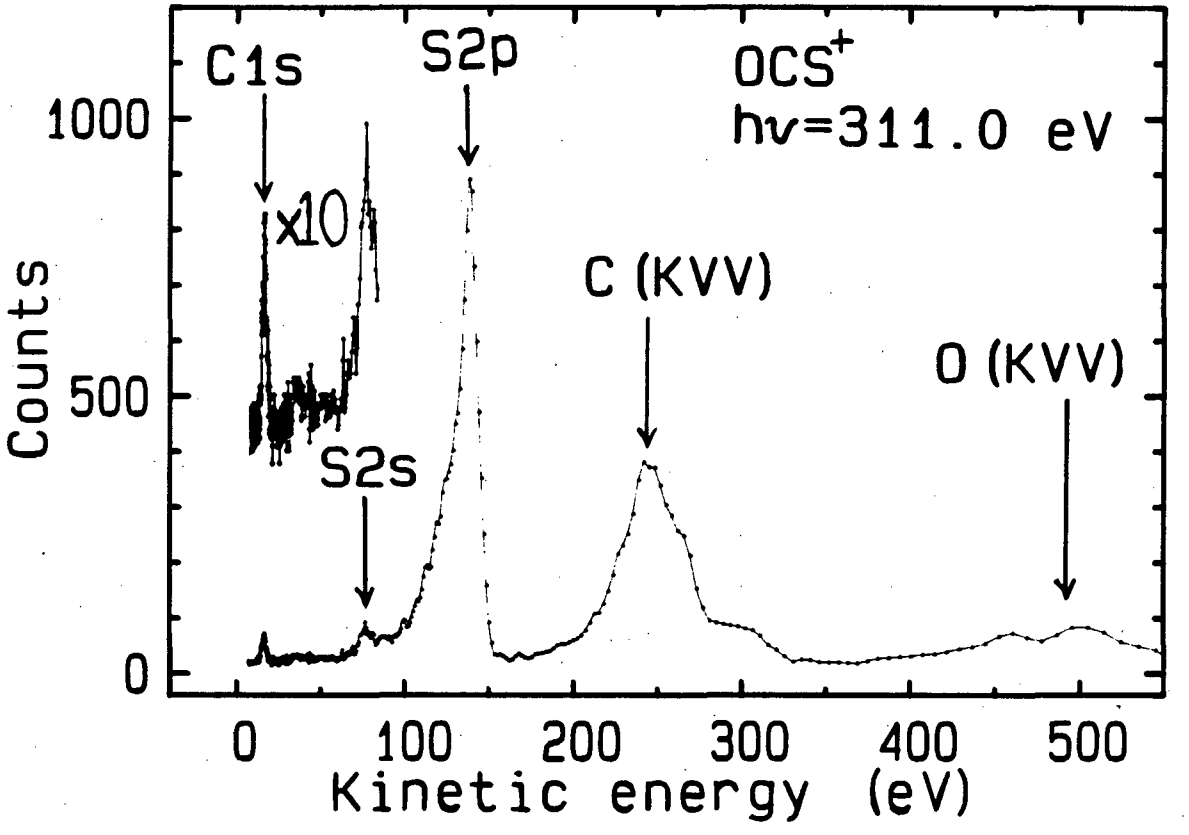
C1s
S2p
OCS+
hν=311.0 eV
x10
C (KVV)
O (KVV)
S2s
Counts
1000
500
0
0
100
200
300
400
500
Kinetic energy (eV)
XBL 832-8335

Figure 18

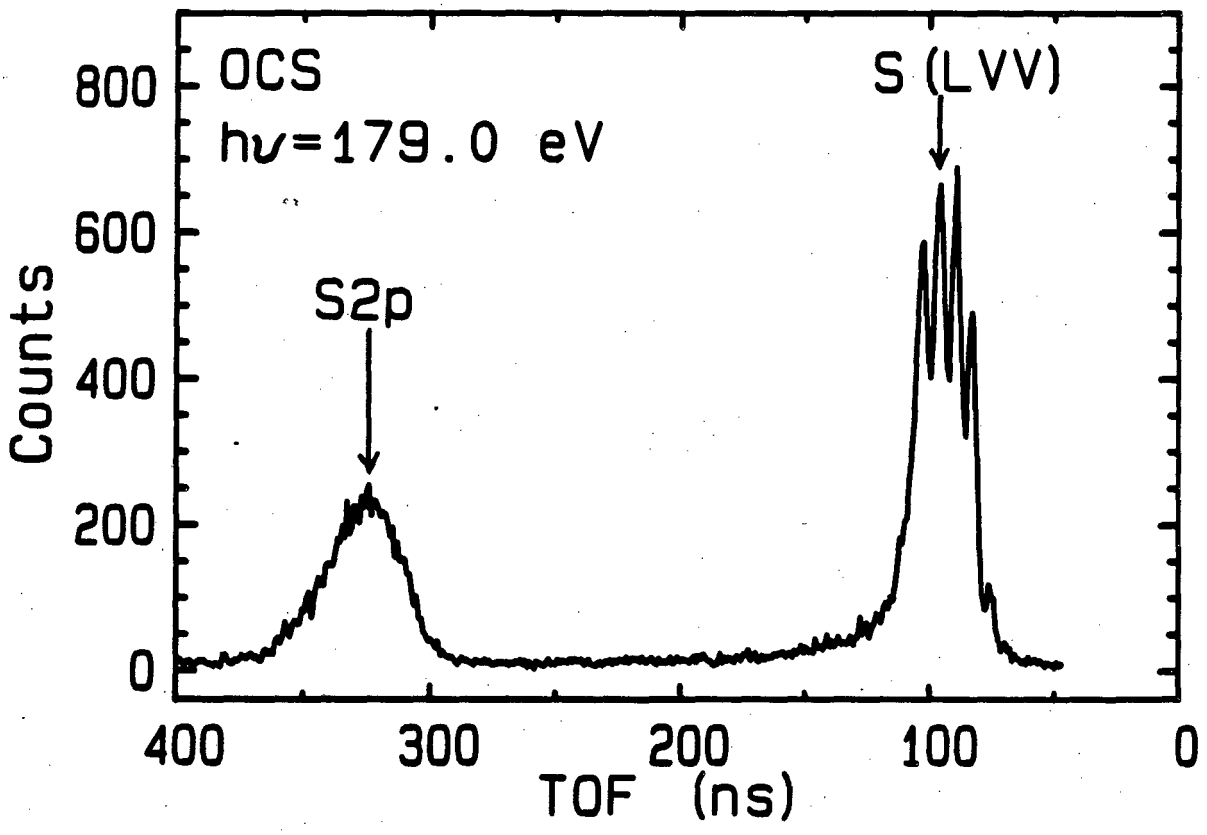

XBL 832-8336

Figure 19

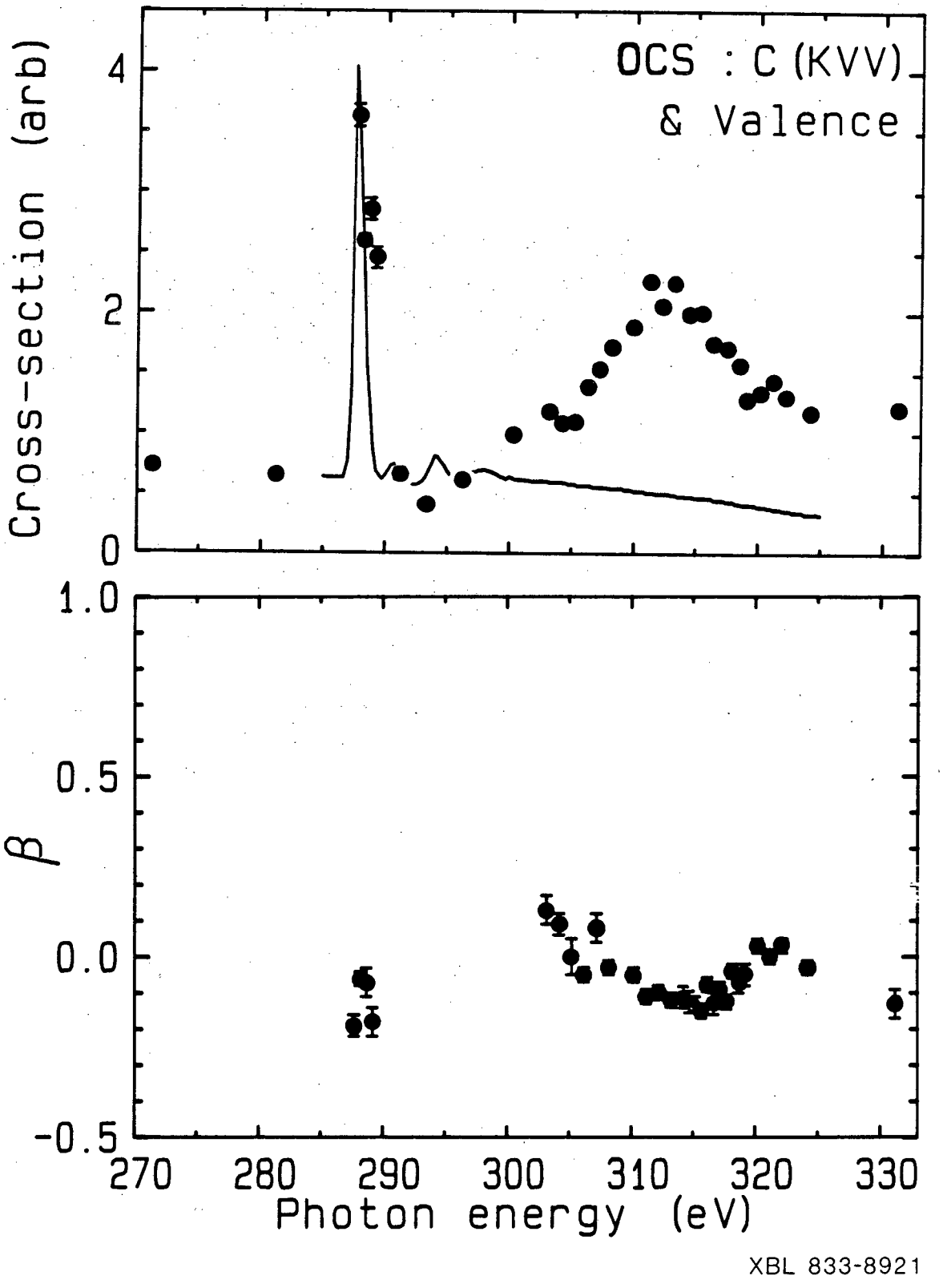
OCS : C (KVV)
& Valence
Cross-section (arb)
4
2
0
1.0
0.5
0.0
-0.5
β
270
280
290
300
310
320
330
Photon energy (eV)
XBL 833-8921

Figure 20

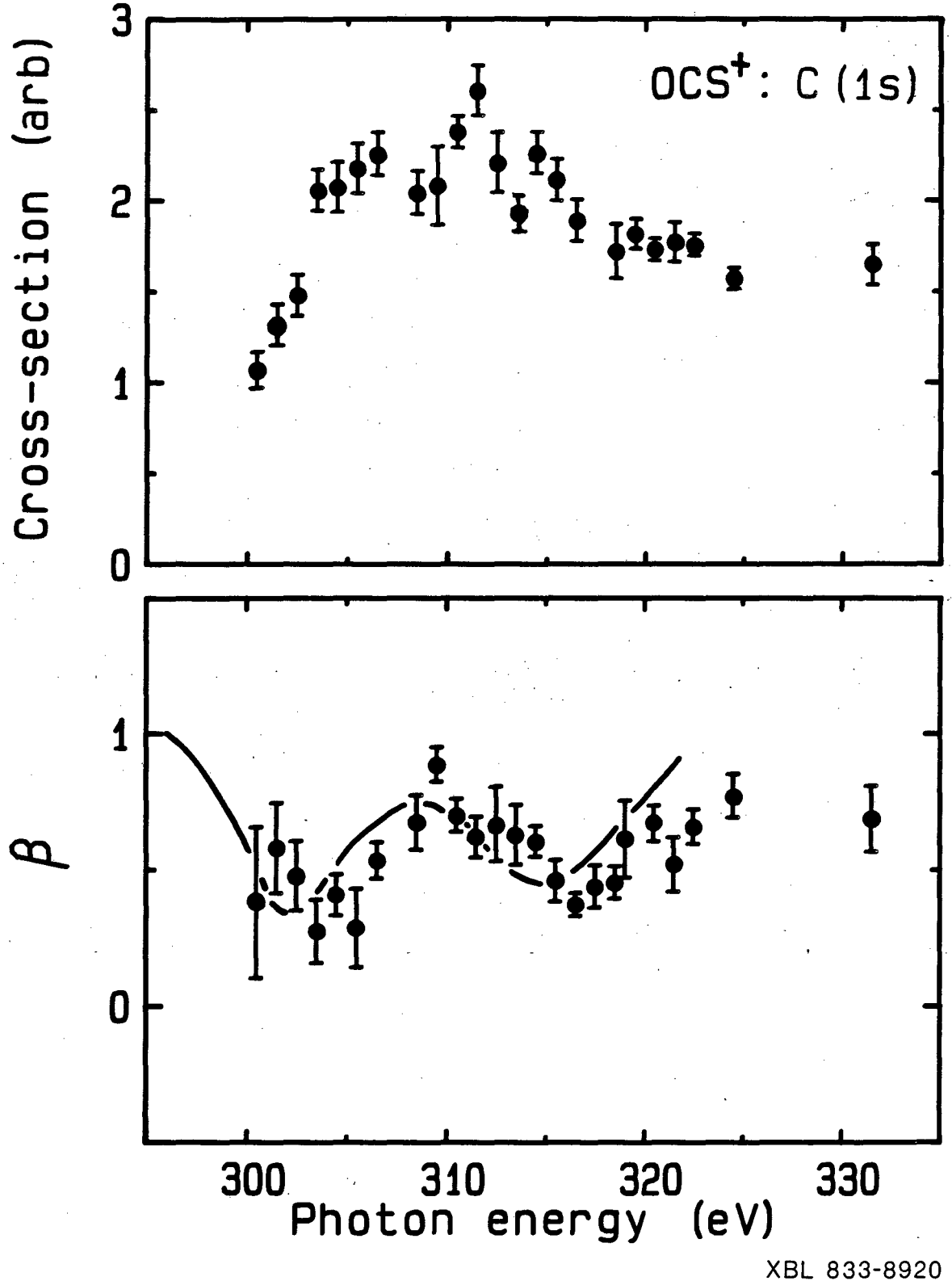
OCS+: C (1s)
Cross-section (arb)
3
2
1
0
β
1
0
300
310
320
330
Photon energy (eV)
XBL 833-8920

Figure 21

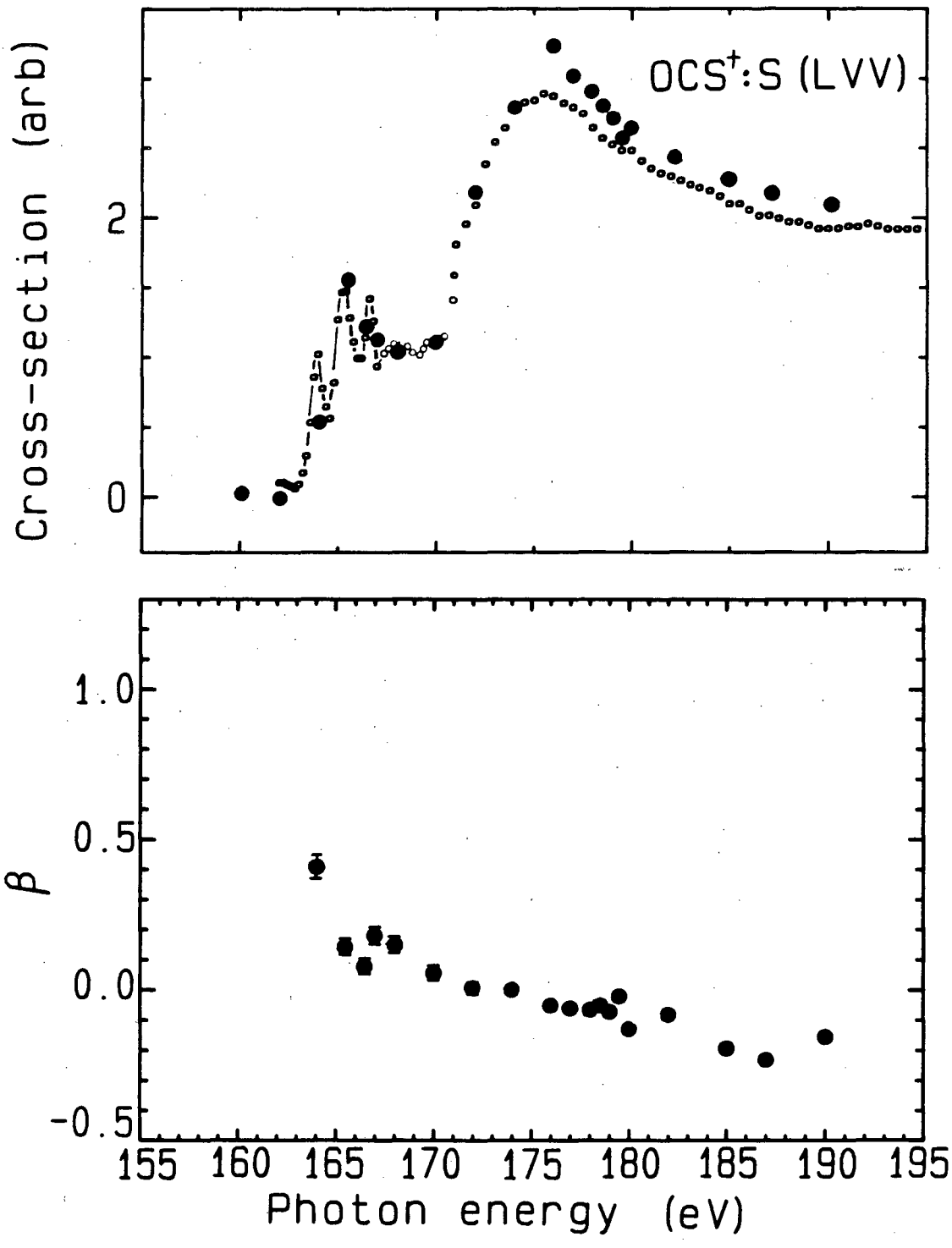
OCS+:S (LVV)
Cross-section (arb)
2
0
β
1.0
0.5
0.0
-0.5
155 160 165 170 175 180 185 190 195
Photon energy (eV)
XBL 828-11147

Figure 22

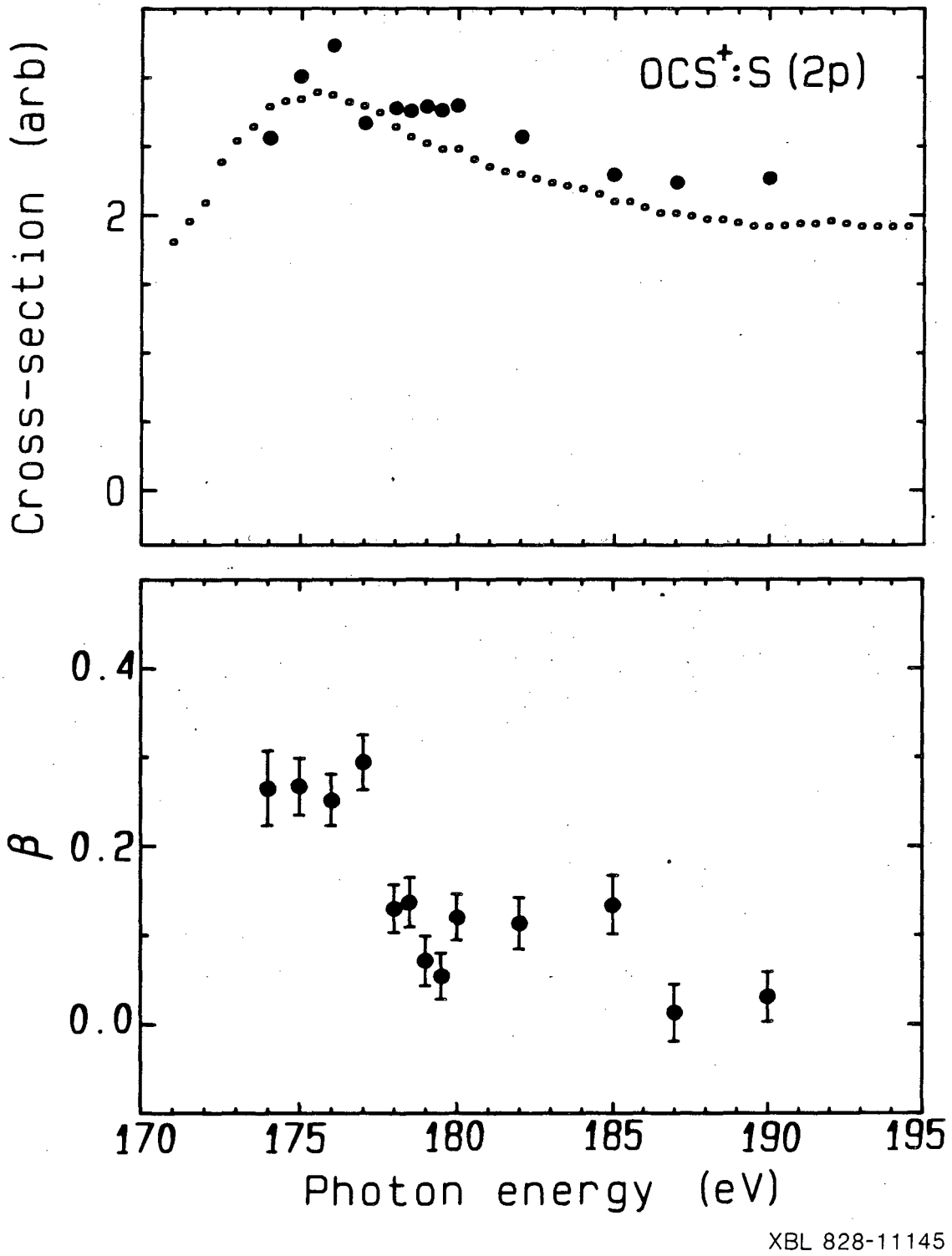
OCS+:S (2p)
Cross-section (arb)
2
0
β
0.4
0.2
0.0
170
175
180
185
190
195
Photon energy (eV)
XBL 828-11145

Figure 23

TECHNICAL INFORMATION DEPARTMENT
LAWRENCE BERKELEY LABORATORY
UNIVERSITY OF CALIFORNIA
BERKELEY, CALIFORNIA 94720